



ISSN: 2800-1729

Edition : Vol 2. Num 1 (2023)

Biopolymer Applications Journal



Editor in chief:

Pr. HAMMICHE Dalila



UNIVERSITÉ ABDERRAHMANE MIRA - BEJAIA
FACULTÉ DE TECHNOLOGIE

Table of content

Rebiha BELLACHE, Dalila HAMMICHE, Amar BOUKERROU

Microencapsulation of olive oil by Poly-hydroxy-butyrates-co-valerate / Polyethylene glycol.
Vol 2, N° 1, 2023, pp. 01-07

Lisa KLAAI, Dalila HAMMICHE, Hassina AOuat, Amar BOUKERROU

Effect of mechanical recycling on the properties of a composite material based on polyvinyl chloride loaded with olive husk flour.
Vol 2, N° 1, 2023, pp. 08-15

Rebiha BELLACHE, Dalila HAMMICHE, Amar BOUKERROU

Preparation of herbal ointments by the method of crushing the flowers.
Vol 2, N° 1, 2023, pp. 16-21

Lisa KLAAI, Dalila HAMMICHE, Hassina AOuat, Amar BOUKERROU

Treated Olive Husk flour in a PVC-Based Composite Material: Recycling Effect on Physico-Mechanical and Rheological Properties.
Vol 2, N° 1, 2023, pp. 22-29

Chahinez MEDJANE, Abdelhakim BENSLIMANE, Nadir MESRATI

Analytical and numerical investigation of displacements and stresses in thick-walled FGM cylinder with exponentially-varying properties.
Vol 2, N° 1, 2023, pp. 30-35

Microencapsulation of olive oil by Poly-hydroxy-butyrate-co-valerate / Polyethylene glycol

Rebiha BELLACHE*, Dalila HAMMICHE, Amar BOUKERROU

Laboratoire des Matériaux Polymères Avancés, Département Génie des Procédés, Faculté de Technologie, Université de Bejaia, Algérie.

Corresponding author email* rebiha.bellache@univ-bejaia.dz

Received: 04 January 2022; Accepted: 24 January 2022; Published: 26 January 2023

Abstract

Encapsulation is a technology widely used in the industrial field because it brings many advantages, especially in the pharmaceutical field. Among the existing microencapsulation techniques, microencapsulation by solvent evaporation in simple emulsion remains one of the most used for hydrophobic active ingredients because it does not require specific equipment and uses mild operating conditions (temperature and ambient pressure generally). Which was the subject of our present study which targets to encapsulation the olive oil by polyhydroxy (butyrate-co-valerate) PHBV using the method of evaporation of the organic solvent which is chloroform. The encapsulation yields obtained with respect to the different parameters are between 66 and 80 %, the best of which is obtained with the highest amount of active ingredient, which is 0.4 g/ml. Microscopy allowed us to observe the morphology of the powders obtained, where the latter are in the form of a powder (spherical) and other are aggregates. The macroscopic and microscopic analysis showed that the increase of the emulsion agitation speed, the amount of surfactant percentage and the nature of the latter, allow to modify the size of the microparticles, which has been proved, in agreement with the theory. The FTIR analysis showed the presence of olive oil in the PHBV microparticles, and highlighted the absence of chemical interactions between the polymers and olive oil. Thermal analysis by thermogravimetry confirmed the existence of olive oil in the PHBV microparticles by the presence of two losses of mass, first in the interval (200 to 250) which corresponds to the degradation of oil and another loss after this range of (250 to 400) attributed to the decomposition of the encapsulant (PHBV).

Keywords: PHBV, PEG, olive oil, Microencapsulation, physico-chemical properties.

I. Introduction

Polymers and copolymers of lactic and glycolic acids are the most commonly used to develop drug delivery systems due to their safe and authorized use applications in humans [1]. However, other biodegradable polymers have been studied to increase the number of biodegradable materials available for pharmaceutical and medical applications [2]. Poly-hydroxy-butyrate-co-valerate abbreviated usually as PHBV or PHBHV, is naturally occurring biodegradable polymer produced from a wide range of microorganisms [3]. Besides, it is non-toxic, 100% biodegradable, biocompatible with many types of cells, characterized by its high degree of crystallinity, and it is resistant to ultraviolet radiation and acceptable amounts of alcohols, fats, and oils [4] An alternative to giving protection and stability to active compounds is the encapsulation in biopolymers [5], the emulsion solvent evaporation has been the most frequently used microencapsulation method [6].

The oils encapsulation can be defined as a process in which the droplets of the bioactive oil are surrounded by a coating material, or embedded in a homogeneous or heterogeneous matrix, to give small capsules with many useful properties [7]. The oils encapsulation in a practical

system is of potential interest and functional for pharmaceutical, food and cosmetic products [8]. Other important application areas such as personal care, agricultural products, veterinary medicine, industrial chemicals, biotechnology, and biomedical engineering, are all in the biomedical engineering, are all within the range of interest. Because of the wide range of oils in nature, there is growing interest in the application of encapsulating such oils to fully exploit their fully exploit their beneficial benefits [9].

Krishnan et al.(2005) [10], encapsulated Cardamom oil which possesses potential antibacterial, antioxidant, anticancer, antiseptic, antispasmodic, digestive, diuretic and stimulant activities. The microencapsulation is prepared with a mixture of gum arabic, maltodextrin, and modified starch increased volatile stability.

Umesha et al.(2013) [11], encapsulated the garden cress oil (GCO) using different wall materials such as sodium caseinate (SACA), whey protein concentrate (WPC), blend of maltodextrin and gum arabica (MDGA) and skimmed milk powder (SKM) was examined using spray-drying method. In another work of Silva et al. (2014) [12], studied the influence of different combinations of wall materials

and homogenization pressure on the microencapsulation of green coffee oil by spray drying. The encapsulation of this oil facilitates its use in cosmetic powders and reduces the allergenic effects of cinnamic acid when applied directly to the skin.

Lim et al.(2012) [13], established the effects of different wall materials on the physicochemical properties and oxidative stability of spray-dried microencapsulated red fleshed pitaya (*Hylocereuspolyrhizus*) seed oil. This microencapsulation with sodium caseinate and whey protein has increased its stability to oxidation. The chitosan-carrageenan polyelectrolyte complex has been successfully used as an effective matrix to encapsulate neem seed oil by Devi et al.(2009) [14]. Kanakdande et al.(2007) [15], studied microencapsulation of cumin oleoresin by the mixture of gum arabic / maltodextrin / modified starch.

In recent years, olive oil has received great attention owing to its biological activities and sensory qualities. It has social and economical importance for the Mediterranean regions [16]. The importance of olive oil is mainly attributed to its high content of oleic acid and its richness in phenolic compounds, which act as natural antioxidants [17].

For this, in this work, we are interested in the encapsulation of olive oil by polyhydroxy (butyrate-co-valerate) or PHBV using the method of evaporation of the organic solvent which is chloroform, the choice fell on the olive oil as an active principle thanks to its important therapeutic properties, its availability and its low cost compared to other oils which present the same characteristics but with a high cost.

II. Materials and Methods

II.1. Materials

PHBV copolymer used in this work was supplied by TianAn Biologic Materials Co. Ltd (China) with a molar ratio of 92:8 (HB: HV). It was commercialized in the form of pellets under the grade name ENMAT Y1000P.

The olive oil obtained by hot extraction (mountain of bejaia-Algeria).

The PEG used was grade 600 (Mw = 600 g/mol), which acted as a nonionic surfactant, and chloroform used in this study as a solvent was produced by Biochem, chemopharm, (Quebec), were supplied by Biochem Chemopharma (Montreal, Quebec).

II.2. Methods

Preparation of PHBV microcapsules containing olive oil (with different concentrations 0.15g/ml, 0.25 g/ml, 0.4g/ml)

From the calculation of the encapsulation yield for the three concentrations performed (see Table 1), it is deduced that the third concentration 0.4g/ml was the high concentration of the active ingredient (0.4 g/ml) has a better yield of 80% compared to the other concentrations (0.15 and 0.25 g/ml), This can be explained by the influence of the active ingredient on the encapsulation yield. And thus, increasing the amount of olive oil is accompanied by an increase in encapsulation yield.

The encapsulation technique by solvent evaporation was performed according to the following steps:

➤ Preparation of the organic phase (solution 1):

A dissolution of a desired amount of PHBV (1.2 g) in chloroform; add different concentrations (0.15g/ml, 0.25 g/ml, 0.4g/ml) of olive oil to this polymeric solution after cooling in 2 minutes.

➤ Preparation of the aqueous phase (solution 2):

A dissolution of a desired amount of PEG (1 %) in distilled water.

The introduction by drop, of the solution 1 to the solution 2 and leave under agitation;

Medium magnetic stirring is maintained overnight, at room temperature, so that the chloroform is completely removed.

The solution obtained is centrifuged at 6000 rpm for 3 minutes and recovery of the microparticles, then rinsed with distilled water 3 times; Put the microparticles in petri dishes and let dry in a desiccator.

III. Characterizations

➤ Encapsulation yield (R%)

In order to calculate the encapsulation yield we first measured the mass of the microcapsules recovered after centrifugation and is calculated with the following formula:

$$R (\%) = \frac{\text{mass of recovered microcapsules}}{\text{mass of polymer} + \text{mass of olive oil}} * 100$$

This calculation of yield allowed us to deduce which is the best concentration of encapsulation of the active principle by the PHBV.

➤ Macroscopic aspect

The verification of the color and the homogeneity of the various concentrations were carried out by a simple visual analysis for the microparticles obtained.

➤ Microscopic aspect

Optical microscopy allows to obtain information, certainly qualitative, but often essential to the general understanding of the systems.

➤ Structural analysis:

FTIR spectra of the different samples were recorded using Agilent Technologies Cary 630 FTIR in the range of 4000-400 cm⁻¹ with a resolution of 4 cm⁻¹.

➤ Thermal analysis

The thermal study of the samples was conducted using a LINSEIS STAPT 1600-type thermogravimetric apparatus in the range of temperature 20–700°C, and a heating rate of around 10°Cmin⁻¹.

IV. Results and discussion

IV.1. Encapsulation yield (R%)

These results were confirmed by morphological analysis (macroscopic and microscopic aspects).

The HLB or Hydrophilic-Lipophilic Balance is closely related to the structure of the surfactant molecule. Its values are determined according to an arbitrary scale ranging from 0 to 20, it is accepted that emulsifiers with an HLB value between 0 and 8 are lipophilic, those between 8 and 12 are said (intermediate) and those between 12 and 20 hydrophilic [18], and in our study, we used a surfactant

(PEG 600) with HLB = 13. Rabiskova et al. [19] found that the nature of the surfactant affects the oil uptake by the complex coacervate droplets as a function of the HLB value of the surfactant and the addition of surfactants with HLB values between 2 and 6 resulted in maximum uptake of the emulsions into the microcapsules. Although surfactants with HLB values outside this range improve the stability of the emulsions. It adversely modifies the surface properties of the oil droplets and thus prevents encapsulation.

IV.2. Macroscopic aspect

According to the table 2, the low quantity of olive oil used in our experimentation (0.15g/ml), which did not allow the formation of microparticles but rather a formation of aggregates. This result can also be explained by the low


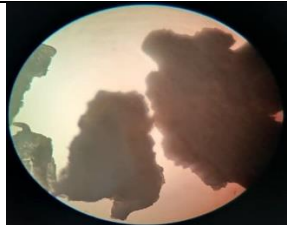
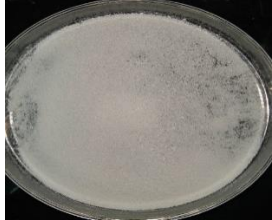
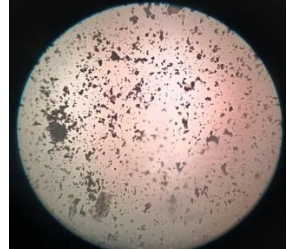

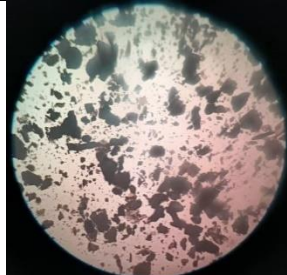
concentration of the surfactant which is insufficient to prevent the coalescence of the emulsion droplets. In this case, the microcapsules agglomerate and form aggregates. A similar finding was reported by Chacon et al.1996 [20], who explained the formation of polymer aggregates during the preparation of PLGA microcapsules containing cyclosporine, by the low concentration of the surfactant which was insufficient to stabilize the emulsion.

According to this, there is a proportional relationship between the concentration of the active ingredient and the size of the microcapsules, i.e. the higher the concentration of olive oil, the greater the increase in the size of the microparticles, which is confirmed by the appearance of the figures of the concentrations of 0.4 g/ml and 0.25 g/ml.

Table 1: The encapsulation yield according to the concentration of olive oil

Concentrations of olive oil (g/ml)	Encapsulation yield (R%)
0.15	66.51
0.25	79.25
0.4	80

Table 2: Macroscopic and Microscopic aspect of microcapsuls

Concentrations of olive oil (g/ml)	Macroscopic aspect	Observations	Microscopic aspect	Observations
0.15		The obtained microparticles are in the form of aggregates and of whitish color.		The presence of aggregates and therefore the absence of homogeneity.
0.25		The microparticles in the form of a fine powder and whitish color.		The presence of microparticles of homogeneous shape.
0.4		Microparticles in the form of a powder of medium granulometry and whitish color.		The presence of microparticles of non-homogeneous shape (large, small and medium).

IV.3. Microscopic aspect

In order to select the best concentration from the morphological point of view (see Table 2), we performed an optical analysis, according to our observation we noticed that the best concentration is 0.4 g/ml; this result was explained by the impacts of the different parameters of encapsulation process.

The stirring speed is the main parameter to control the size of the emulsion droplets. Enhancing the stirring speed generally results in the decrease of the average diameter of the microcapsules [21], [22].

According to the study by André-Abrant et al [22], the size of microcapsules decreases from 281µm to 91µm when the stirring speed is enhanced from 300 to 700 rpm. Similar

results were found by Valot et al [21] who showed that the size of microcapsules prepared with two polymers (Eudragit and EC), decreases when the stirring speed is enhanced.

The composition of the solvent is a factor influencing the final size of the microcapsules which has been proven by Kim et al [23] and Maia et al [2]. Have proven that the use of solvent with high solubility in water in combination To confirm the presence of olive oil in PHBV microcapsules and to study the interactions that may be established between PA and polymer, the FTIR spectra of virgin PHBV olive oil, and PHBV microcapsules containing olive oil were recorded between 400 and 4000 cm^{-1} . The FTIR spectrum of PHBV (see Figure 1) revealing the presence of several absorption bands, in particular [24] :

A rather narrow peak located at 3440 cm^{-1} characteristic of the elongation vibration of the -OH bond.

A series of bands with peaks centered at 2965, 2940 and 2875 cm^{-1} ; attributed respectively to the vibrations of asymmetric elongation of the CH_3 group, symmetric

with low soluble solvents decreases the size of the obtained particles. For Kim et al. 2005[23] the average sizes of poly(ϵ -caprolactone) microspheres resulting from the use of dichloromethane are 73.5 μm compared to those obtained with a mixture of dichloromethane and ethyl formate which are 56.6 μm .

IV.4. Structural analysis

elongation of the CH_2 group and symmetric elongation of CH_3 .

A very intense band centered at 1750 cm^{-1} attributed to the elongation of the $\text{C}=\text{O}$ carbonyl group of the esters.

A very broad band of peaks at 1445, 1390 and 1290 cm^{-1} corresponding respectively to the deformation vibrations of CH_3 , to the elongation of the $\text{C}=\text{O}$ group of the esters, to the vibration of the C-O-H bond.

A series of peaks 1000 and 800 cm^{-1} characteristic of the elongation vibrations of the C-C bonds.

Figure 2 presents the FTIR spectrum of olive oil reveals the presence of several absorption bands, which are cited in the following table 3[25]:

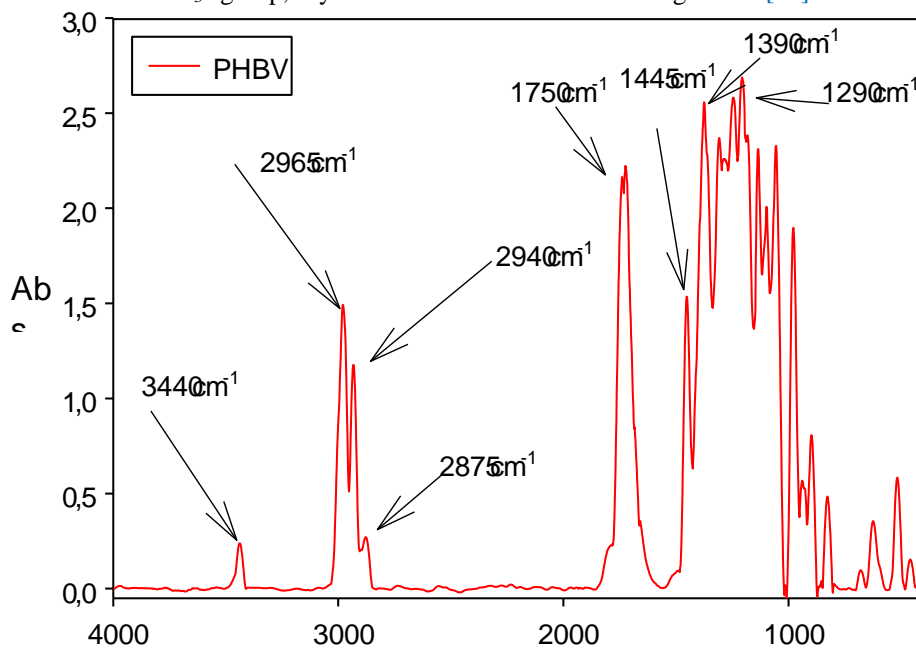


Figure 1: FTIR of PHBV

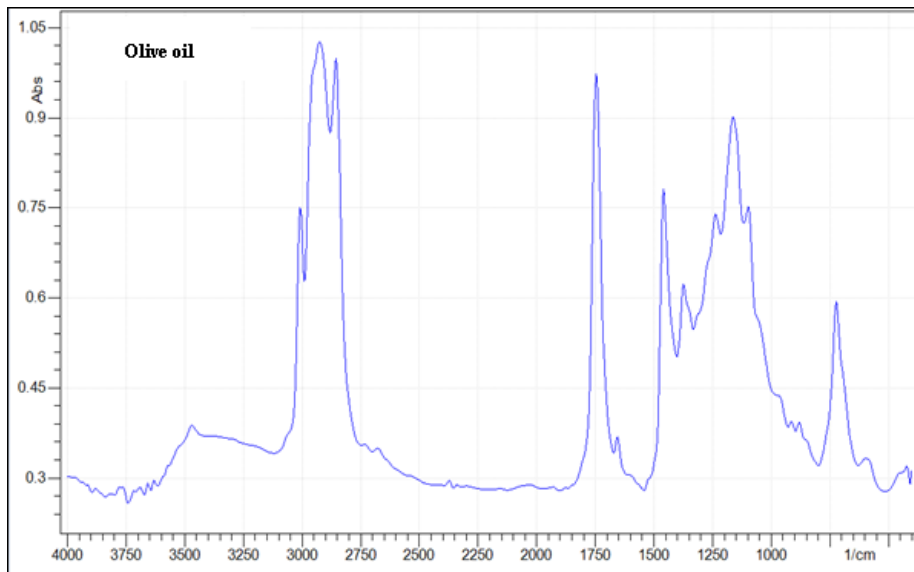


Figure 2: FTIR of Olive oil

Table 3: FTIR of Olive oil

Band (cm ⁻¹)	Functional group	Intensity
3464	(C=O)	Weak peak
3005	(=C-H) cis	Medium
2922	(C-H) CH ₃	Very strong
2852	(C-H) CH ₂	Very strong
1742	(C=O) ester	Very strong
1652	(C=C)	Weak
1459	(C-H) CH ₂	Medium
1238 and 1162	(C-O)	Medium
961	(C-O)	Weak
898 and 839	-HC-CH-	Weak

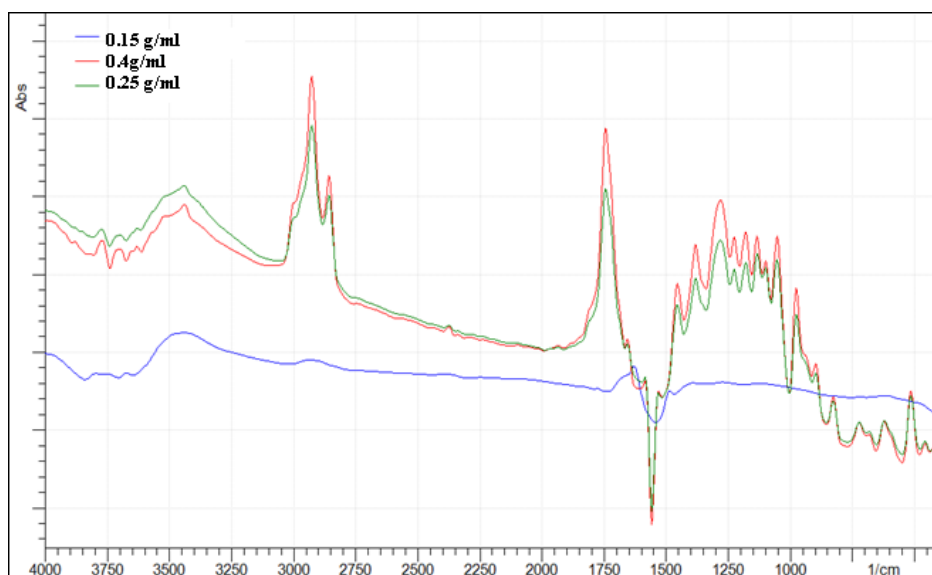


Figure 3: FTIR of PHBV/olive oil microcapsules in different concentrations

From the FTIR spectrum of PHBVmicroparticles containing olive oil(Figure 3):

- A broad band located in the 3464 area characteristic of the olive oil ester group C=O.

- A band located in the area of the peaks centered around 3000 to 2875 cm^{-1} ; of the CH_2 group that occurred in PHBV and the CH band in olive oil
- A new peak at 2338, which signifies the formation of $\text{C}\equiv\text{C}$ triple bonds correspond to the aromatic ring of the active ingredient.
- An intense peak located at 1725 cm^{-1} features the $\text{C}=\text{O}$ band, which presented in PHBV and in olive oil and thus the presence of the latter in the PHBV matrix.

We also notice that the intensity of concentration 0.4g/ml is stronger than concentration 0.25g/ml and to this effect; we can say that the encapsulation of olive oil with concentration 0.4g/ml is slightly better than that of concentration 0.25g/ml.

It is also observed that all the bands of PHBV appear in the spectrum of microparticles without any change in wave number, this indicates that the integrity of the active

ingredient is preserved after the encapsulation process. This leads us to assume that the active ingredient remains stable and that there are no chemical interactions between the active ingredient and the polymer studied.

IV.5. Thermal analysis

According to the figure 4 and table 4, we observe successively:

A first loss of mass from 80°C to about 100°C, which is perhaps attributed to the evaporation of water, then directly another loss at about 200°C to 250°C, which is probably related to the degradation of olive oil or the active principle used.

The second loss of mass is located from 300°C, it corresponds to the degradation of the PHBV biopolymer. This result confirms the presence of olive oil in the PHBV microcapsules, which has been verified by other previous analysis[26].

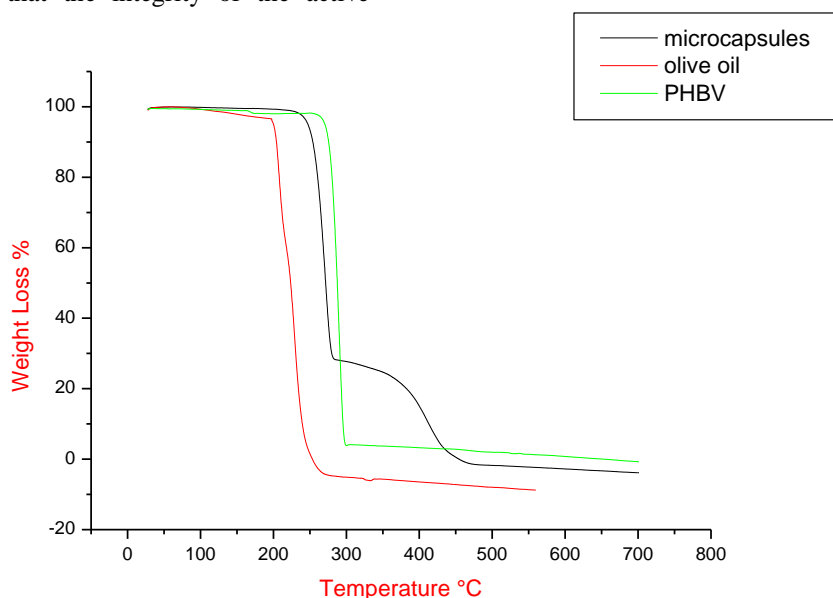


Figure 4 : Thermograms of PHBV, olive oil and microcapsules

Table 4: The onset temperature and Tmax of PHBV, Olive oil and PHBV/ Olive oil microcapsules

Samples	Ti (°C)	Tmax (°C)
PHBV	262	290
PHBV/ Olive oil microcapsules	239	300
Olive oil	196	253

V. Conclusions

The work presented is part of a research program that has set as an objective to prepare microparticles by the technique of emulsion evaporation of the solvent from biodegradable and biocompatible polymeric matrices. The active ingredient chosen for this study is olive oil, the polymers used are the PHBV as a base matrix and PEG as active tension.

- The encapsulation yields obtained with respect to the different parameters are between 66 and 80 %,

the best of which is obtained with the highest amount of active ingredient which is 0.4 g/ml.

- The microscopy allowed us to observe the morphology of the powders obtained, where the latter are in the form of a powder (spherical) and other are aggregates.
- The FTIR analysis showed the presence of olive oil in the PHBV microparticles, and highlighted the absence of chemical interactions between the polymers and olive oil.

- Thermal analysis by thermogravimetry confirmed the existence of olive oil in the PHBV microparticles by the presence of two losses of mass, first in the interval (200 to 250) which corresponds to the degradation of oil and another loss after this range of (250a 400) attributed to the decomposition of the encapsulant (PHBV).

Acknowledgements

The authors would like to thank the students "OUHNIA Thinhineneand IBELHOULEN Kahina" in polymer engineering of process engineering department, university of Bejaia.

Disclosure of interest: The authors report no conflict of interest.

References

- [1] D. Chulia, M. Deleuil, and Y. Pourcelot. Powder Technology and Pharmaceutical Processes. Elsevier Science B V Amsterdam, 557, 1994.
- [2] J.L. Maia, M.H.A. Santana, M.I. Ré. The effect of some processing conditions on the characteristics of biodegradable microspheres obtained by an emulsion solvent evaporation process. Braz. J. Chem. Eng., 21, 01–12, 2004.
- [3] A. A. Chowdhury. Poly-3-hydroxybuttersure abbauende Bakterien und Exoenzym. Arch. For Mikrobiol, 47,(2). 167-200, 1963.
- [4] R. Bellache, D. Hammiche, A. Bettache, et A. Boukerrou. Enzymatic degradation of prickly pear seed (PPS)/Polyhydroxy(butyrate-co-valerate) (PHBV) biocomposite. Materials Today Proceedings, 53, 113-116, 2022.
- [5] E. Franceschi. Precipitation of β -carotene and PHBV and co-precipitation from SEDS technique using supercritical CO₂. J. Supercrit. Fluids, 47 (2), 259-269, 2008.
- [6] E. T. Baran, N. Özer and V. Hasirci. Poly(hydroxybutyrate-co-hydroxyvalerate) nanocapsules as enzyme carriers for cancer therapy: an in vitro study. J. Microencapsul., 19 (3), 363-376, 2002.
- [7] L. Sagalowicz and M. E. Leser. Delivery systems for liquid food products. Current Opinion in Colloid & Interface Sciences, 15, 61–72, 2010.
- [8] L. Sanguansri, L. Day, Z. Shen, P. Fagan, R. Weerakkody, L. J. Cheng. Encapsulation of mixtures of tuna oil, tributyrin and resveratrol in a spraydried powder formulation. Food & Function, 4, 1794–1802, 2013.
- [9] R. Abdallaoui. La microencapsulation des huiles : meilleure approche pour la valorisation des produits alimentaires, doctorat thesis maroc, 2018.
- [10] S. Krishnan, R. Bhosale, R.S. Singhal. Microencapsulation of cardamom oleoresin: evaluation of blends of gum arabic, maltodextrin and a modified starch as wall materials. Carbohydrate Polymers 61:95–102, 2005.
- [11] S.S. Umesha, B. Monahar, K.A. Naidu. Microencapsulation of alpha-linolenic acid-rich garden cress seed oil: physical characteristics and oxidative stability. Eur J Lipid Sci Technol, 115:1474–82, 2013.
- [12] V.M. Silva, G.S. Vieira, M.D. Hubinger. Influence of different combinations of wall materials and homogenisation pressure on the microencapsulation of green coffee oil by spray drying. Food Research International, 61:132–43, 2014.
- [13] H.K. Lim, C.P. Tan, J. Bakar, S.P. Ng. Effects of different wall materials on the physicochemical properties and oxidative stability of spray-dried microencapsulated red-fleshed pitaya (Hylocereus polyrhizus) seed oil. Food Bioprocess Technol 5:1220–7, 2012.
- [14] N. Devi, T.K.Maji. A novel microencapsulation of neem (Azadirachta indica A. Juss.) seed oil (NSO) in polyelectrolyte complex of kappa-carrageenan and chitosan. J Appl Polym Sci 113:1576–83, 2009.
- [15] D. Kanakdande, R. Bhosale, R. S. Singhal. Stability of cumin oleoresin microencapsulated in different combination of gum arabic, maltodextrin and modified starch. Carbohydrate Polymers 67:536–41, 2007.
- [16] M. De Luca, W. Terouzi, G. Loele, F. Kzaiber, A. Oussama, F. Oliverio, R. Tauler, G. Ragno. Derivative FTIR spectroscopy for cluster analysis and classification of morocco olive oils, Food Chemical. 124; 1113–1118, 2011.
- [17] Bendini, A., Cerretani, L., Carrasco-Pancorbo, A., Gómez-Caravaca, A. M., Segura-Carretero, A., Fernández-Gutiérrez, A. Phenolic molecules in virgin olive oils: a survey of their sensory properties, health effects, antioxidant activity and analytical methods. An overview of the last decade. Molecules, 12, 1679–1719, 2007.
- [18] A. Harlay, A. Huard, L. Ridoux, V. Rolland. Guide du préparateur en pharmacie. Edition Masson, gondé sur noireau, 791, 2004.
- [19] M. Rabiskova and J. Valaskova. The influence of HLB on the encapsulation of oils by complex coacervation. J. Microencapsul, 15, 747, 1998.
- [20] M. Chacon, L. Berges, J. Molpeceres, M.R. Aberturas, M.Guzman. Optimized preparation of poly D, L (lactic-glycolic) microspheres and nanoparticles for oral administration. Int. J. Pharm, 141, 81-91, 1996.
- [21] P. Valot, M. Baba, J. M. Nedelec, N. Sintes-Zydowicz. Effects of process parameters on the properties of biocompatible Ibuprofen-loaded microcapsules. Int. J. Pharm, 369, 53–63, 2009.
- [22] A. André-Abrant, J.L. Taverdet, J. Jay. Microencapsulation par évaporation de solvant. Eur. Polym. J., 37, 955-963, 2001.
- [23] B.K. Kim, S.J. Hwang, J.B. Park, H.J. Park. Characteristics of felodipine-located poly(epsilon-caprolactone) microspheres. J. Microencapsul, 22, 193–203, 2005.

- [24] R. Bellache, D. Hammiche, A. Boukerrou. Physico-chemical characterization of hydrolytic Degradation of Prickly Pear Seed enhanced Poly-Hydroxy (Butyrate-co-Valerate) biocomposite. *Macromolecular Symposia.*, 404, 2100371, 2022.
- [25] R. Bellache, D. Hammiche, A. Boukerrou. Elaboration of ointments based on vegetable plants “*Calendula arvensis*” and “*Dandelion*”. *Biopolymer Applications Journal*, 1(2), 01-07, 2022.
- [26] R. Bellache, D. Hammiche, A. Boukerrou, B. S. Kaith. Prickly pear seed oil (PPSO) encapsulated by biodegradable polymer Poly-hydroxy-butyrate-co-valerate (PHBV). <https://doi.org/10.1016/j.matpr.2022.11.441>. p.791.

Effect of mechanical recycling on the properties of a composite material based on polyvinyl chloride loaded with olive husk flour

Lisa Klaai*, Dalila Hammiche; Hassina Aouat ; Amar Boukerrou

Laboratoire des Matériaux Polymères Avancés (LMPA), Faculté de Technologie, Université de Bejaia, 06000 Bejaia, Algérie

Corresponding author* lisa.klaai@univ-bejaia.dz

Received: 04 January 2022; Accepted: 24 January 2022; Published: 26 January 2022

Abstract

In this article, we try to contribute to the development of methods and strategies necessary to transform olive husk (OH) from waste for disposal into valuable raw materials as bio-filler for the PVC, for providing a composite with very high physical-mechanical and thermal characteristics interesting. Several formulations of composite materials based on PVC (as a matrix), olive husk (as filler) and a PVC-g-MA coupling agent, have been the subject of study experiments to assess the structural-mechanical and thermal properties. Investigate the combined effect of olive husk flour, PVC-g-MA and recycling on composite properties.

The results showed that the mechanical properties of the composites increase with the number of extrusion cycles, the tensile strength and the Young's modulus in the studied formulations increased considerably. On the other hand, the infrared spectra show no significant change after four extrusion cycles. It is also important to take into account the evolution of the thermal properties of the composites after the transformation cycles. We noticed that the addition of olive husk flour causes a slight decrease in the temperature of onset of degradation.

Keywords: Lignocellulosic flour, Polyvinyl chloride, recycling, mechanical properties, thermal behavior.

I. Introduction

Nowadays, the need to preserve the environment and save energy has become more than necessary for the future of the planet. In the face of this, environmental degradation and climate change affect humanity. The development of plant resources produced by the Algerian soil provides a very interesting alternative to environmental problems and the probable depletion of fossil resources. Olive pomace, one of these natural resources, is a by-product of waste from various oil mills. Every year, thousands of tons of this product are incinerated or simply released into nature, causing major inconvenience for the environment [1,2]. It is the abundance of this waste that motivated the choice of olive husk flour as feedstock in the manufacture of composite materials.

Natural fiber composite materials occupy an important place in the history of technology. The increasing use of vegetable fibers as reinforcements in composites with thermosetting or thermoplastic matrices provides very interesting environmental advantages. However, the strongly hydrophilic

nature of the fiber weakens the interfacial bond with the hydrophobic matrices but this problem of incompatibility has been resolved by the development of original techniques for improving adhesion, the various techniques tried can be divided into two categories: physical modification methods and chemical methods [3-5].

Composites are increasingly used in many industrial fields such as aeronautics, automotive, shipbuilding, infrastructure, etc. Indeed, they have many advantages compared to conventional materials reside in their performance, lightness and in particular good mechanical properties combined with low density, ease of handling during implementation and low production cost. Environmental concerns, both in terms of limiting the use of fossil resources and the need to manage the waste produced, have led to increased pressure to recycle materials [6,7]. The options available for waste disposal and management are recycling and/or reuse in different useful products.

Nadali et al [8]. were emphasized on closed-loop recycling of wood flour/poly (vinyl chloride) composites, since there is normally a considerable

amount of material waste in wood plastic production lines. Composite materials were produced and subjected to four times reprocessing cycles under industrial conditions. Detailed analytical methods including bending strength, modulus of elasticity, impact strength, scanning electron microscopy, fiber length, water absorption, contact angle, Fourier transform infrared, and dynamic mechanical thermal analysis (DMTA) were conducted to evaluate the effects of recycling on the mentioned composites. Results demonstrated that the recycled composites, except for the four-time recycled ones, had lower bending strength, modulus of elasticity, and impact strength due to fiber-chain scission/fracture resulting from shear stress during reprocessing; however, impact strength remained almost unchanged after the first recycling cycle. Results also revealed that generally the reprocessed composites showed lower water absorption rates due to better fiber wetting and encapsulation. There was also a reduction in hemicellulose hydroxyl groups, rendering the recycled composites less hydrophilic. DMTA results showed an increase in mechanical loss factor ($\tan \delta$) for all the reprocessed composites showing a more viscous than elastic nature. The glass transition temperature of fourth cycle composites increased due to polymer dehydrochlorination and the resulting cross-linking, which restricted the molecular mobility of the polymer chains.

According to Augier et al [9], twenty extrusion-milling cycles of internal waste of poly (vinyl chloride) (PVC) and wood fiber-reinforced PVC composite were performed and the mechanical and thermal properties evaluated. This comparison provided evidence of the influence of the vegetable fibres on the thermo-mechanical degradation of the composite material. Up to five cycles, the composite properties remained stable. But after 10 cycles and especially at 20 cycles, the flexural strength increased, whereas the other mechanical properties remained almost constant. At the same time, a decrease of the degradation temperature revealed a deterioration of the molecular structure. The PVC properties remained constant, whereas a great increase in the impact strength was observed after 20 cycles without deterioration of the molecular structure. The different behaviors between the composite and the PVC were explained by the influence of the fibres, which accelerated the PVC degradation, characterized by

dehydrochlorination followed by crosslinking reactions.

The study done by Lakhdar et al. [10] was carried out experimentally on three bio-loads of which the chicken feathers are the best of them. The other two bio-loads (cow horns and coconut) decrease elongation at break and also increase rigidity. Adding 10% chicken feathers to the recycled PVC improves flexibility by recovering elongation length at break, and stiffness by reducing stress at break. For these recoverable values, we will be sure to increase the recyclability number of PVC.

This study aims the development of a composite material from the combination of olive husk flour as a filler with PVC as a thermoplastic matrix in the presence of a coupling agent, PVC-g-MA, to improve the interfacial adhesion, which helps to obtain ultimate mechanical and thermal properties.

II. Material and methods

II.1 Material

The used Polyvinyl chloride (PVC), type SE-1200, has K-Wert value of 70.20 to 72.00, viscosity value of 0.99-1.030 and a density of 0.481-0.561

The main additives of PVC were summarized in table 1.

Table 1: Additives of PVC SE-1200

Additives	Names	Value (%)
Plasticizer	Dioctyl Phthalate (DOP)	30
Stabilizer	Ca/Zn	4
Lubricant	Stearic Acid	0.5

The filler used was olive husk flour; it was obtained after olives processing for oil in the region of Bejaia (Algeria). The olive husk has sustained several pre-treatments, namely washing with hot water to eliminate pulp, drying under ambient conditions for 48 h, grinding, and sieving to have a grain size of $\leq 100 \mu\text{m}$ [11].

PVC-g-MA was synthesized at the laboratory of organic materials A. Mira University of Bejaia, Algeria by Hammiche et al [12]. The addition of a coupling agent aims for interfacial adhesion improvement.

II.2 Methods

Preparation of composites

The mixtures are made using a Brabender type mixer, Plasticorder W 50 EHT. The PVC-g-MA compatibilizers and the olive husk flour are first steamed at 60°C for 24 hours. The various

constituents are mixed manually then introduced into the Brabender for 5 min, at a temperature of 180° C. and a rotation speed of 50 rpm.

Mass compositions of the various formulations are given in Table 2.

Table 2: Mass composition of the different formulations

	PVC compound (%)	OHF (%)	PVC-g-MA (%)
PVC	100	0	0
PVC/OHF	80	20	0
PVC/PVC-g-MA/OHF	75	20	5

The processed samples are recycled four times in the internal mixer. These are characterized after each transformation cycle.

Fourier Transform Infrared Spectroscopy (FTIR)

The IR spectra of the virgin PVC and the composites were recorded on a SHIMADZU model FTIR-8400S spectrophotometer, driven by a computer equipped with processing software with a resolution of 4 cm⁻¹, in the region between 4000 cm⁻¹ and 400cm⁻¹.

Tensile test

The tensile test allows us to determine the behavior of a material under the effect of a constraint as well as its nature (rigid or flexible). The tensile tests of the PVC/OHF composites were carried out on an MTS synergy RT1000 type tensile machine at ambient temperature (23° C.) and a displacement speed of 2 mm/min. In this study, the results presented are the average of five trials for each sample.

Thermogravimetric analysis (ATG/DTG)

The thermograms of the different samples were recorded using a mettler-type thermogravimetric device, consisting of an ATG/DTG/ATD coupled and plotted by a microcomputer, it is composed of a sample boat of 10 at 30 mg, the boat is introduced into an oven in an inert nitrogen medium with a heating rate of 10° C./min in an interval ranging from 20° C. to 700° C.

III. Results and discussion

Fourier Transform Infrared Spectroscopy (FTIR)

The FTIR spectra of the PVC, PVC/OHF and PVC/PVC-g-MA/OHF formulations at the 1st and 4th transformation cycles are illustrated in figure 1.

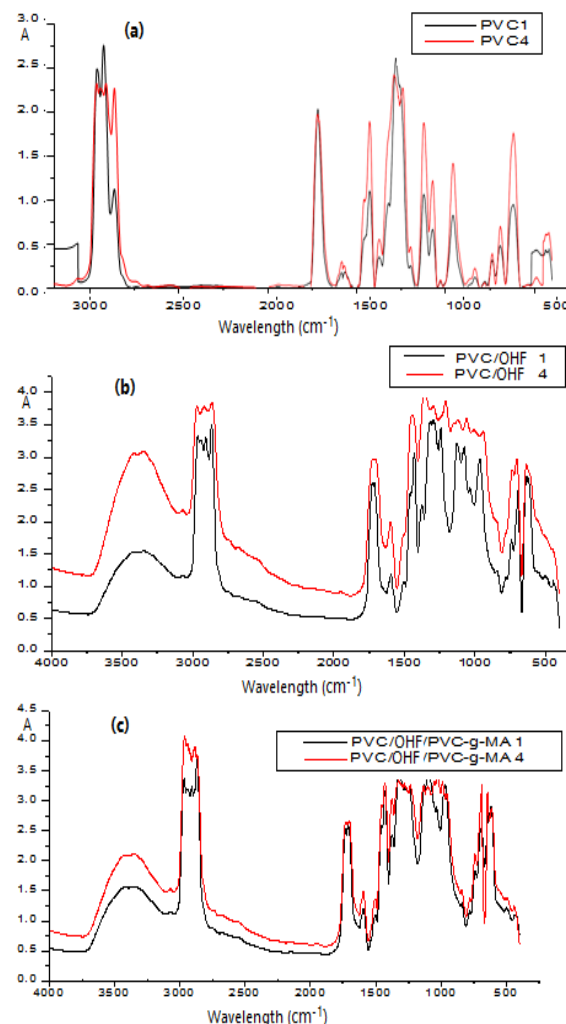


Figure1: FTIR spectra of (a) PVC, (b) PVC/OHF and (c) PVC/PVC-g-MA/OHF formulations at the 1st and 4th transformation cycles.

The FTIR spectra of virgin PVC and composites with and without compatibilizers reveal the presence of an absorption band located at 1735cm⁻¹ which can be associated with the carbonyl stretching of the acetyl, aldehyde, carboxyl and ester groups contained in hemicelluloses, lignin and extracts [13]. Moreover, a broad absorption band is observed at 3350 cm⁻¹ in composite PVC/OHF samples, which is attributed to the hydroxyl groups contained in the cellulosic of the olive husk flour. The localized absorption band at about 1600–1630 cm⁻¹ is probably associated with absorbed water in crystalline cellulose [14]. After four extrusion cycles no significant change was observed in the infrared spectra of PVC in the carbonyl region

1700-1850 cm^{-1} which are generated by the oxidative degradation of polyolefin during recycling [15]. We observed a slight increase in carbonyl concentration for composites with and without PVC-g-MA. Similar results are found in the literature [16-18].

Tensile test

Figure 2 illustrates the evolution of (a) Young's modulus, (b) tensile strength and (c) elongation at break as a function of the number of transformation cycles of PVC, PVC/OHF and PVC/PVC-g-MA/OHF formulations.

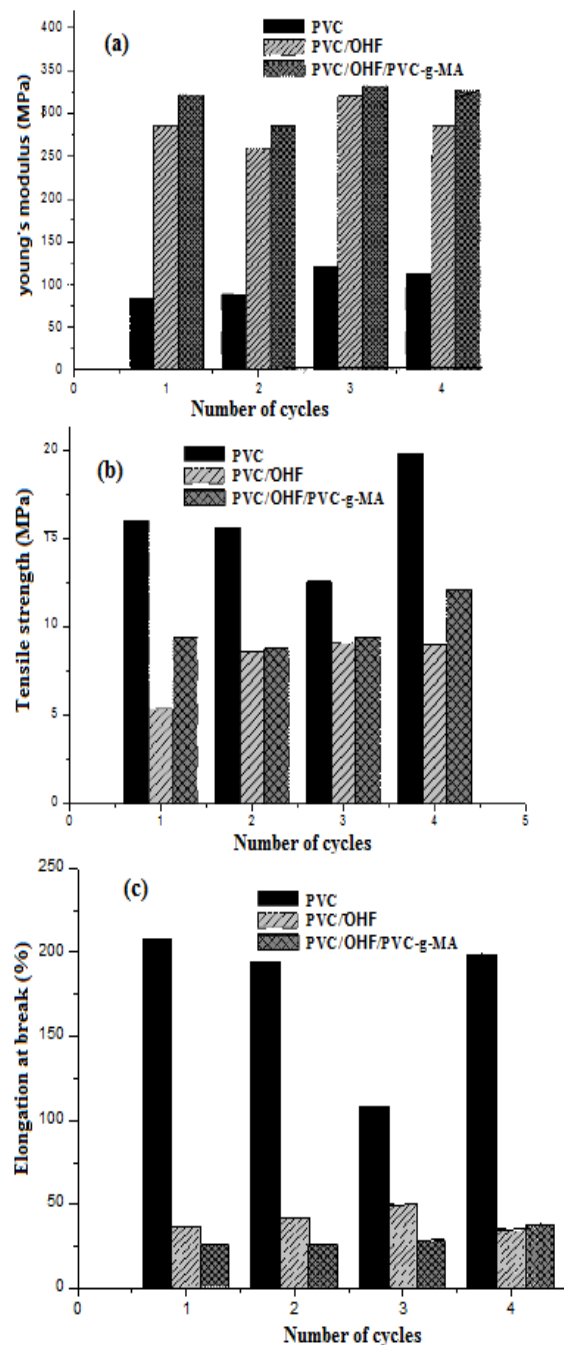


Figure 2: evolution of (a) Young's modulus, (b) tensile strength and (c) elongation at break as a function of the number of transformation cycles of PVC, PVC/OHF and PVC/PVC-g-MA/OHF formulations.

During the first transformation cycle, a significant increase in Young's modulus is recorded with the addition of the charge. However, this increase is more remarkable in the presence of PVC-g-MA.

The Young's modulus of the composites show a strong increase induced not only by the reduction in the dimension of the fibers caused by the grinding but also by their good dispersion and therefore an improvement in the interfacial adhesion between the matrix and the reinforcement, especially in the presence of PVC-g-MA and in the third transformation cycle [19,20].

On the other hand, we observed a reduction in the tensile strength of the composites compared to virgin PVC.

The increase in PVC stress is less marked with recycling, there is a slight decrease in stress in the first cycle then an increase in this property in the fourth cycle, and this is probably due to the crosslinking of PVC induced by the setting in implementation [21,22].

However, the increase in the tensile strength of PVC/OHF and PVC/PVC-g-MA/OHF composites is recorded going from 5.4MPa, 9.4MPa respectively in the first cycle to 9MPa, 12.1MPa in the 4th cycle and this is due to a better dispersion of the fiber in the matrix which was due to the reduction of the melt viscosity [23,24].

It is observed that the elongation at break of the PVC matrix is less affected by recycling; it is around 208% in the first processing cycle and 198% in the fourth processing cycle. The addition of the olive husk fiber to the PVC matrix significantly reduces the elongation at break and this is due to the stiffness induced by the vegetable fiber. Generally, the addition of lignocellulosic filler causes a significant decrease in the ductility of the composite [25].

Thermogravimetric analysis (TGA/DTG)

Thermogravimetric analysis makes it possible to follow the variation of the mass of a sample as a function of temperature.

Figure 3 represents the (a) TGA, (b) DTG thermograms obtained from the various virgin PVC, PVC/olive husk and PVC/olive husk/PVC-g-MA formulations during the 1st transformation cycle.

It is noted that the decomposition of PVC occurs in two stages the first stage begins at 270°C and ends around 365°C with a maximum temperature of degradation in the vicinity of 300°C corresponding to a speed of the order of 30% / min and 70% mass loss which is attributed to the dehydrochlorination of PVC and volatile products which consist mainly of HCl, small amounts of benzene, toluene and other hydrocarbons. After this step, the chlorine has been almost completely eliminated. This means that at low temperatures most of the chlorine can be removed from PVC, which forms the basis for other PVC treatment processes. The elimination of HCl molecules lead to the formation of double bonds along the macromolecular chains of PVC, hence obtaining a new polyacetylene polymer [26].

Between 365°C and 415°C, the sample becomes thermally stable, i.e. it does not lose weight at this temperature interval. The second step is linked to the degradation of polyacetylene between 415-520°C to form a residue consisting of carbon black [27]. However, we note that the addition of olive pomace fiber causes a slight decrease in the temperature at which degradation begins, they are of the order of 254°C, 245°C for composites without and with PVC- g-MA respectively, the decrease in decomposition onset temperature for composites treated with PVC-g-MA is due to improved interfacial interaction between the fiber and the matrix by generating strong ester bonds between them [12].

The decomposition of composites takes place in three stages, an exothermic peak located between 250 and 320°C, which corresponds to the thermal depolymerization of hemicelluloses and pectin's, a major secondary decomposition around 390-420°C attributed to the decomposition of cellulose , a last peak representing the decomposition of the residues [28].

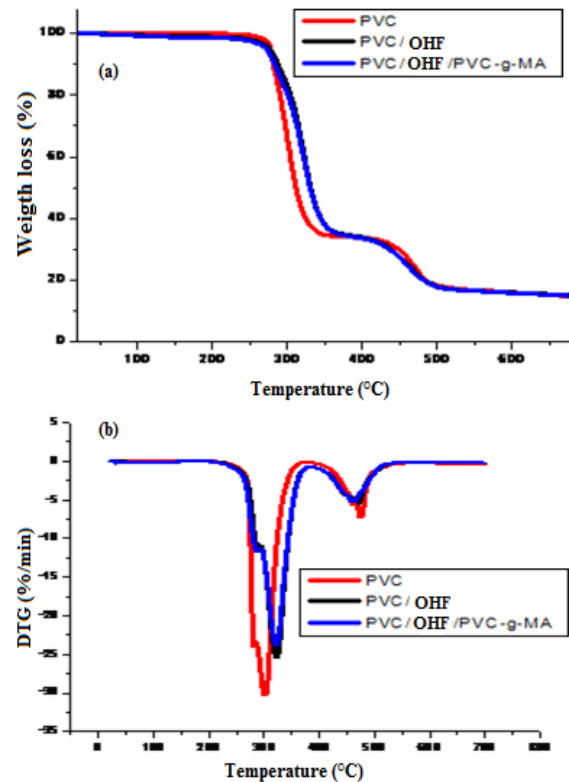


Figure 3: the (a) TGA, (b) DTG thermograms obtained from the various virgin PVC, PVC/olive husk and PVC/olive husk/PVC-g-MA formulations during the 1st transformation cycle.

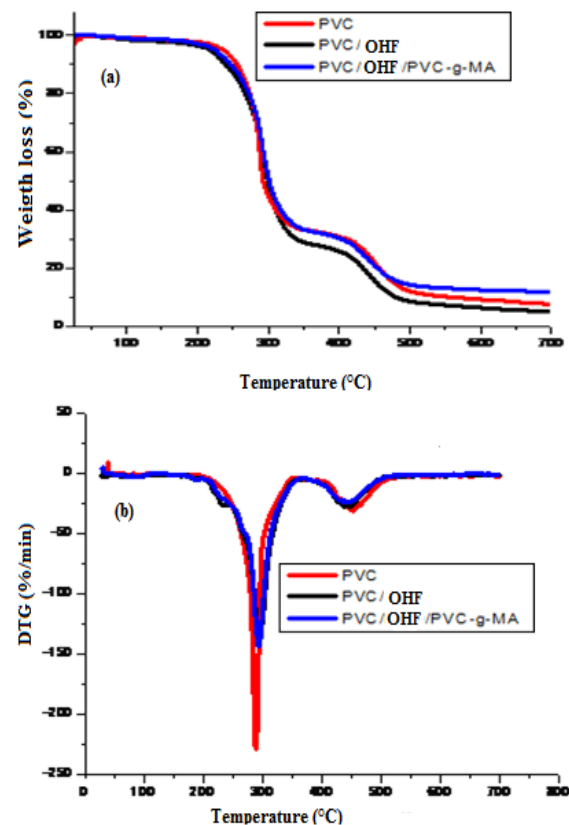


Figure 4: (a) TGA, (b) DTG thermograms of virgin PVC and PVC/OHF, PVC/OHF/PVC-g-MA composites at the fourth recycling cycle.

Figure 4 Represents the (a) ATG, (b) DTG thermograms of virgin PVC and PVC/OHF, PVC/OHF/PVC-g-MA composites at the fourth recycling cycle. We note a decrease in the temperature at which degradation begins compared to composites at the 1st recycling cycle, in fact it is 220°C for virgin PVC and 205°C for composites with and without PVC-g-MA. This decrease is followed by a very rapid decomposition of PVC compared to composites with and without PVC-g-MA. Similarly, we note the decrease in temperature at $T_{50\%}$ of PVC and composites in the fourth cycle and this is due to the increase in molecular weight of PVC and composites.

Contrary to the results of Beg et al [29], weight loss positions on ATG thermograms for PP and composites shifted towards higher temperatures with increasing transformation cycle number, suggesting an increase in thermal stability which is probably due to the increase in crystallinity of PP resulting from the reduction in molecular weight.

The DTG thermograms also show that the maximum rate of degradation of virgin PVC is higher than that of composites, however this parameter decreases according to the number of transformation cycles[30,31].

VI. Conclusions

In conclusion, the aim of this work is to study the mechanical and thermal properties of PVC/olive husk composites with and without PVC-g-MA according to the number of recycling they have undergone.

The results showed that the mechanical properties of the composites increase with the number of extrusion cycles, the tensile strength and the Young's modulus in the studied formulations increased considerably. On the other hand, the infrared spectra show no significant change after four extrusion cycles.

It is also important to take into account the evolution of the thermal properties of the composites after the transformation cycles. We noticed that the addition of olive husk flour causes a slight decrease in the temperature of onset of degradation. So it plays an important protective role; by slowing down its rate and speed of degradation.

Overall this study indicates that PVC/olive husk flour composites represent a good quality for use after multiple recycling especially in the presence of the accounting agent.

Conflict of interest

The authors declare that they have no conflict for financial interests or personal relationships that how

can influence the work reported in this paper.

References:

- [1] H. Boussehel. Etude de moyens stabilisation des composites à base de polystyrène .Thèse doctorat, Université de Biskra, 2018.
- [2] L. Klaai, D. Hammiche, A. Boukerrou, J. Duchet-Rumeau, J.F. Gérard, N. Guermazi. On the use of prickly pear seed fibres as reinforcement in polylactic acid biocomposites. *Emergent Materials*, 5, 859-872, 2022
- [3] A. Boukerrou, M. Beztout, H. Djidjelli, S. Krim, D. Hammiche. The effect of chemical treatment of cellulose with epoxidized soybean oil (ESO) on the properties pvc/cellulose composites. *Molecular Crystals and Liquid Crystals*, 556,223–232, 2012 .
- [4] L. Klaai, D. Hammiche, A. Boukerrou, V. Pandit. Thermal and Structural Analyses of Extracted Cellulose from Olive Husk. *Journal of Materials Today: Proceedings* 52,104–107,2022
- [5] L. Klaai, D. Hammiche, A. Boukerrou, F. Arrakhiz. Assessment of natural cellulosic fibers derived from agricultural by-product. *Journal of Materials Today: Proceedings* 53, 260-264, 2022
- [6] Z. Hruska, Patrice Guesnet, Christian Salin, J-J Couchoud. Poly (chlorure de vinyle). *Technique de l'ingénieur (AM 3325)*. France, 2007
- [7] L. Klaai, D. Hammiche, H. Ibrahim, A. Boukerrou. Hydrolytic aging of a biopolymer reinforced with Alfa fiber treated with dispersing agent. *Biopolymer Applications Journal* 1,06-12, 2022
- [8] E. Nadali , R. Naghdi. Effects of multiple extrusions on structure–property relationships of hybrid wood flour/poly (vinyl chloride) composites. *Journal of Thermoplastic Composite Materials* 35, 1076-1093,2022

- [9] L. Augier, G. Sperone, C. Vaca-Garcia, M.E. Borredon. Influence of the wood fibre filler on the internal recycling of poly(vinyl chloride)-based composites. *Polymer Degradation and Stability* 92, 1169-1176, 2007
- [10] A. Lakhdar, A. Moumen, K. Moumen. Experimental study of the mechanical effect of bio-loads on PVC recycling. *Journal of Applied Engineering Science* 20, 221 - 229, 2022
- [11] H. Aouat, D. Hammiche, A. Boukerrou, H. Djidjelli, Y. Grohens, I. Pillin. Effects of interface modification on composites based on olive husk flour. *Materials Today: Proceedings* 36, 94-100, 2021
- [12] D. Hammiche, A. Boukerrou, H. Djidjelli, M. Beztout, S. Krim. Synthesis of a new compatibilisant agent PVC-g-MA and its use in the PVC/alfa composites. *Journal of Applied Polymer Science* 124, 4352-4361, 2012
- [13] H. Boulahia, A. Zerizer, Z. Touati, A. Sesbou. Recycling the Cork Powder in a PVC-Based Composite Material: Combined Effect on Physico-Mechanical and Thermal Properties. *International Polymer Processing* 31, 346-355, 2016
- [14] Y. Cui, S. Lee, B. Noruziaan, M. Cheung, J. Tao. Fabrication and interfacial modification of wood/recycled plastic composite materials. *Composites: Part A*, 39, 655, 2008.
- [15] M. H. Martins, M. A. De Paoli. Polypropylene compounding with post-consumer material: II. Reprocessing. *Polymer Degradation and Stability* 78,491, 2002
- [16] K.L. Pickering, M.G. AruanEfendy, T.M. Le. A review of recent developments in natural fibre composites and their mechanical performance. *Composites: Part A* 83, 98-112, 2016.
- [17] E.M. Fernandes, V.M. Correlo, J.A.M. Chagas, J.F. Mano, R.L. Reis. Cork Based Composites Using Polyolefin's as Matrix: Morphology and Mechanical Performance. *Composites Science and Technology* 70, 2310 -2318, 2010
- [18] D. Hammiche, A. Boukerrou, H. Djidjelli, Y.M. Corre, Y. Grohens, I. Pillin. Hydrothermal Ageing of Alfa Fiber Reinforced Polyvinylchloride Composites. *Construction and Building Materials* 47, 293 -300, 2013
- [19] I. Janajreh, M. Alshrah, S. Zamzam. Mechanical recycling of PVC plastic waste streams from cable industry: A case study. *Sustainable Cities and Society* 18, 13-20, 2015
- [20] M. Jammoukh, K. Mansouri, B. Salhi, B. Industrial and ecological effect of a bio-load on polymers. *Materials Today: Proceedings* 13, 939-948, 2019
- [21] M. Sah, M. Hanafi. Mechanical Properties of Coconut Shell Powder Reinforced PVC Composites in Automotive Applications. *Journal of Mechanical Engineering* 14, 49-61, 2017
- [22] G . Guerrica-Echevarria, J.I. Eguiazabal, J. Nazabal. Effects of reprocessing conditions on the properties of unfilled and talc-filled polypropylene. *Polymer Degradation and Stability* 53, 1-8, 1996.
- [23] I. Aranberri, S. Montes, I. Azcune, A. Rekondo, H.J. Grande. Fully Biodegradable Biocomposites with High Chicken Feather Content. *Polymers* 9, 593, 2017
- [24] A. Moumen, M. Jammoukh, L. Zahiri, K. Mansouri. Numerical modeling of the thermo mechanical behavior of a polymer reinforced by horn fibers. *International Journal of Advanced Trends in Computer Science and Engineering* 9(4), 6541-6548, 2020
- [25] M. N. Islam, M. R. Rahman, M. M. Haque, and M. M. Huque. Physico-mechanical properties of chemically treated coir reinforced polypropylene composites. *Composites Part A* 41, 192-198, 2010
- [26] J. Yu, L. Sun, C. Ma, Y. Qiao, H. Yao. Thermal degradation of PVC: A review. *Waste Management* 48, 300-314, 2016.
- [27] J. Nisar, M. S. Khan, M. Iqbal, A. Shah, G.M. AliSayed, T. Mahmood. Thermal decomposition study of polyvinyl chloride in the presence of commercially available oxides catalysts. *Advances in Polymer Technology* 37,2336-2343, 2018
- [28] M. Pracella, D.Chionna, I.Anguillesi Z. Kulinski, E.Piorkowska. Functionalization, compatibilization and properties of polypropylene composites with hemp fibres. *Composite Science and Technology* 66, 2218-2230, 2006.

- [29] M. D. H. Beg, K. L. Pickering. Reprocessing of wood fibre reinforced polypropylene composites Part I: Effects on physical and mechanical properties. *Composites Part A: Applied Science and Manufacturing* 39, 1091–1100, 2008
- [30] S. Bhattacharjee, M.H. Sazzad, M.A. Islam, M.M. Ahtashom, Asaduzzaman, and M.Y. Miah. Effects of fire retardants on jute fiber reinforced polyvinyl chloride/polypropylene hybrid composites. *International Journal of Materials in Engineering Applications* 2,162-167, 2013.
- [31] S.C. Rizzi, D.J. Heath, A.G.A. Coombes, N. Bock, M. Textor, S. Downes. Biodegradable polymer/hydroxyapatite composites: Surface analysis and initial attachment of human osteoblasts. *Journal of Biomedical Materials Research* 55,475-486, 2001

Preparation of herbal ointments by the method of crushing the flowers

Rebiha BELLACHE*, Dalila HAMMICHE, Amar BOUKERROU

Laboratoire des Matériaux Polymères Avancés, Département Génie des Procédés, Faculté de Technologie, Université de Bejaia, Algérie.

Corresponding author email* rebiha.bellache@univ-bejaia.dz

Received: 15 January 2022; Accepted: 24 January 2022; Published: 27 January 2023

Abstract

The present work aims to elaborate the ointments prepared by the method of grinding the flowers of plant calendula arvensis and dandelion. The subject has been reinforced by characterizations namely physical analysis by measuring pH, conductivity and water resistance test, chemical analysis by infrared spectroscopy and morphological analysis (visually and microscopically). From the results, we noticed that in the macroscopic characterization, a semi-solid consistency and homogeneity for the two ointments prepared by the method of grinding the flowers of two plants: calendula arvensis and Dandelion. Microscopically, the both ointments (CAO and DO) have a better physical stability; the latter is characterized by a homogeneous appearance, which was obtained. The yellow flowers ointment DO shows a better chemical stability than the CAO orange flower by the presence of increase of intensity in all the characteristic bands, which confirmed by FTIR analysis, finally, both ointments are water resistant, which was confirmed by the test of water resistance .

Keywords: herbal ointment, crushing flowers, beeswax, olive oil, physico-chemical analysis.

I. Introduction

In English scientific ethnobotanical literature, most of the field studies conducted in Southern Europe and in the entire Mediterranean basin have been based on the traditional uses of medicinal plants within a single cultural context [1]. The need for an effective, safe and economical alternative therapeutic system that can prevent development of resistant microorganisms, and opportunistic infections has become critical. The increases in adverse effects in conventional medicines have navigated researchers towards safe herbal medicinal products. Phytotherapy refers to the alternative system of medicine, which uses plant products, herbs and shrubs for the management of diseases [2]. The components in plants that are having anti-inflammatory [3], analgesic, astringent, antioxidant, antibacterial and anti-fungal properties are called phytochemicals [4].

This plant contains several bioactive compounds, including terpenoids and terpenes (mainly bisabolol, faradiol, chamazulene, arnidiol and esters), carotenoids (mainly with rubixanthin and lycopene structures), flavonoids, (mainly quercetin, isorhamnetin and kaempferol aglycones) and polyunsaturated fatty acids, (mainly calendic acid) [5]. Today, many products essentially cosmetic and pharmaceutical [6] contain *calendula arvensis* and even *Dandelion*, like ointments and creams, and avoid chemical synthesis products that cause irritation and skin diseases [7].

The present work aims at valorizing some work on the elaboration of ointments prepared by the method

of grinding the flowers of plant calendula arvensis and dandelion. The subject has been reinforced by characterizations namely physical analysis by measuring pH, conductivity and water resistance test, chemical analysis by infrared spectroscopy and morphological analysis (visually and microscopically).

II. Materials and Methods

II.1. Materials

The flowers of Calendula arvensis and Dandelion were collected on the campus of the University of Bejaia-Algeria. Beeswax olive oil are of the natural raw materials used in this work [7].

II.2. Methods

The following steps summarize the preparation of calendula arvensis and Dandelion ointments (see Figure 1):

- Carry out a drying of the flowers of the calendula in an oven regulated at a temperature of 45°C during four days (04), then chop the latter to have a fine powder.
- Melt the wax added with olive oil in a water bath until you have a homogeneous oily solution, then add the powder obtained to the liquid and let it simmer 15 minutes while stirring.
- Pour the mixture into a cheesecloth to filter, squeeze the mixture to extract as much liquid as possible.

- Quickly pour the liquid ointment into jars and close them without forcing.
- Once the preparation has cooled, screw the lids on tightly. The ointment obtained must be kept away from heat and light for about 3 months.



Figure 1: A- *calendula arvensis* powder, B- Beeswax with olive oil, C-the addition of plants powder into Beeswax with olive oil, D- Ointment prepared

III. Analysis

- **The pH measurements and conductivities:** Measurement of pH and conductivity of obtained ointments and olive oil.
- **Morphological aspect** (macroscopically and microscopically aspect): provide information on the homogeneity of our ointments.
- **Chemical analysis:** FTIR spectra of the different samples were recorded using Agilent Technologies Cary 630 FTIR in the range of $4000-400\text{ cm}^{-1}$ with a resolution of 4 cm^{-1} .
- **Water resistance:** we have deposited a droplet of water on thin layer of ointment; the photos were taken of the different samples using an optical microscopy.

IV. Results and discussion

IV.1. Measurement of pH and conductivity

According to the obtained results of table 1 of pH [8] and conductivity values, the pH of DO is more than of CAO, and at the same time its conductivity is superior to that of CAO, which can be explained by the displacement of ions [7], [9]. i.e. the increase of the pH led to the enhancement of the conductivity.

IV.2. Macroscopic aspect

According to the results obtained from the macroscopic characterization shown in the Figure 2, a semi-solid consistency and homogeneity for the two ointments prepared by the method of grinding the flowers of two plants: *calendula arvensis* and *dandelion* [10].

IV.3. Microscopic aspect

According to the Figure 3 prepared ointments have a better physical stability; the latter is characterized by a homogeneous appearance, which was found for all prepared ointments of CA and D [11].

According to the results of figure 4, the characteristic bands of the different ointments that show the same appearance are summarized in the table. According to the results obtained from the ointments. The yellow flowers ointment DO shows a better chemical stability than the CAO orange flower by the presence of increase of intensity in all the characteristic bands.

IV.4. Chemical analysis by FTIR

Table 1: Measurement of pH and conductivity of ointments

Samples	pH	Conductivity(µs/cm)
Olive oil	6.82	2.80
Dandelion ointment (DO)	5.45	3
Calendula arvensis ointment (CAO)	5.3	2.5

Dandelion ointment (DO)



Calendula arvensis ointment (CAO)



Figure 2 : Macroscopic aspect of CAO and DO (Before and after application on the skin)

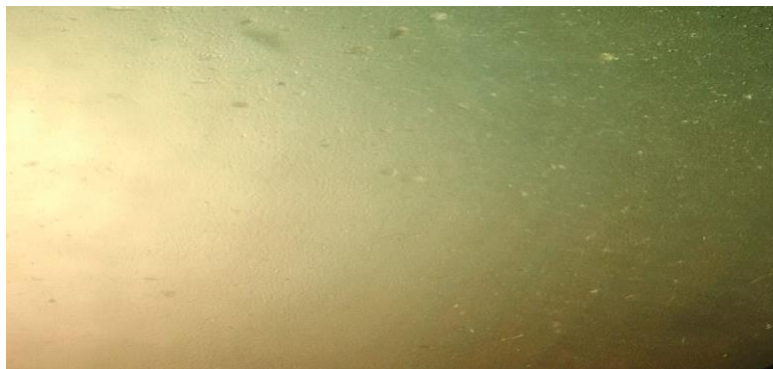


Figure 3 : Microscopic aspect of CAO and DO

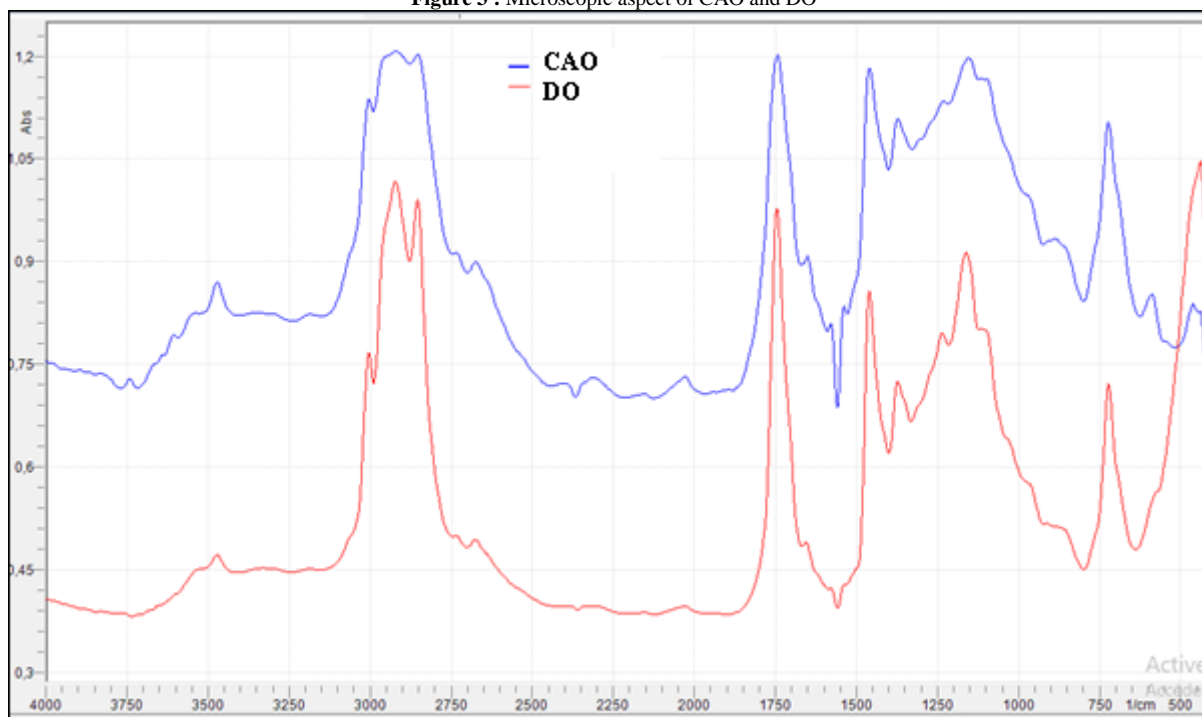


Figure 4: FTIR spectrum of the DO and CAO

Table 2: peak values and functional groups observed for orange flower (CAO) and yellow flower (DO).

Bands (cm ⁻¹)	Fonctionnel groups
3475.86	O-H
3005.64	C-H
2925.70	C-H
2855.17	C-H
2668.96	C-H
1737.93	C=O
1471.78	C=C
1374.92	O-H
1152.03	C-O-
717.55	-CH ₂ -

IV.5. Water resistance

Concerning the Figure 5, The both ointments prepared according to the adapted protocol are non-

miscible, non-adherent on the skin and have an almost spherical shape, especially for the yellow DO flowers. Therefore, both ointments are water resistant.

Dandelion ointment (DO)



Calendula arvensis ointment (CAO)

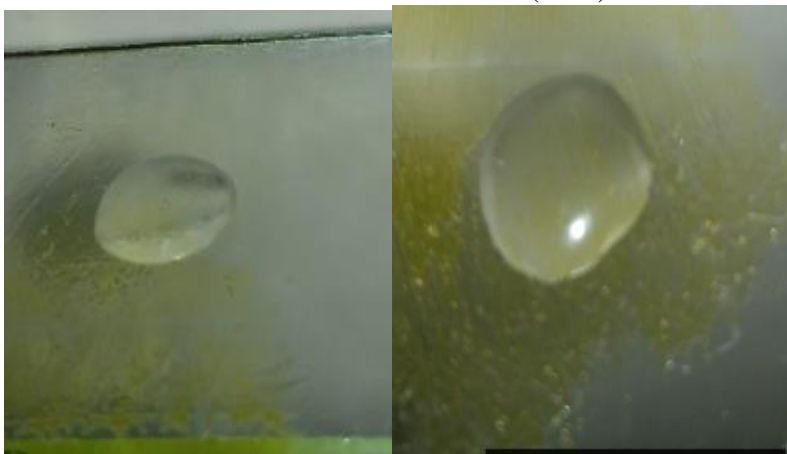


Figure 5: Water resistance of CAO and DO

V. Conclusions

The results obtained constitute a more relevant scientific justification for the traditional use of Calendula arvensis and Dandelion, confirming once again the reliability and effectiveness of traditional remedies in the treatment of numerous ailments.

From the results, we noticed that in the macroscopic characterization, a semi-solid consistency and homogeneity for the two ointments prepared by the method of grinding the flowers of two plants: calendula arvensis and Dandelion. Microscopically, the both ointments (CAO and DO) have a better physical stability; the latter is characterized by a homogeneous appearance, which was obtained. The yellow flowers ointment DO shows a better chemical

stability than the CAO orange flower by the presence of increase of intensity in all the characteristic bands, which confirmed by FTIR analysis, finally, both ointments are water resistant, which was confirmed by the test of water resistance .

Acknowledgements

The authors would like to thank the students "LETRECHE Yasmina and BELAID Kahina" in pharmaceutical engineering of department of process engineering, university of Bejaia.

Disclosure of interest: The authors report no conflict of interest.

References

- [1] M.T. Palmese, R.E.Uncini Manganelli, P.E. Tomei,. An ethnopharmacobotanical survey in the Sarrabus district (south-east Sardinia). *Fitoterapia*. 72, 619–643, 2001.
- [2] P Gardiner. Factors associated with herb and dietary supplement use by young adults in the United States. *BMC Complement Altern Med*. 2007; 7:39.
- [3] C. A. Williams, F. Goldstone, J. Greenham. Flavonoids, cinnamic acids and coumarins from the different tissues and medicinal preparations of *Taraxacum officinale*. *Phytochemistry* 42, 121–127, 1996.
- [4] Gambhir. Herbal medicines and dentistry. *International Journal of Green Pharmacy*.; 10 (3), 2016.
- [5] S. Agatonovic-Kustrin, O.D. Babazadeh, D.W. Morton, A.P. Yusof. Rapid evaluation and comparison of natural products and antioxidant activity in calendula, feverfew, and German chamomile extracts. *Journal of Chromatography*. 1385, 103–110, 2015.
- [6] R. Bellache, D. Hammiche, A. Boukerrou. Prickly pear seed: from vegetable fiber to advanced applications: A review, *Biopolymer applications journal*. 1(1), 01-06, 2022.
- [7] R. Bellache, D. Hammiche, A. Boukerrou. Elaboration of ointments based on vegetable plants “*Calendula arvensis*” and “*Dandelion*”. *Biopolymer Applications Journal*. 1 (2), 01-07, 2022.
- [8] K. Bene, D.Camara, A.Soumahoro i. Y.Kanga, G.N.Zirihi. Formulation galénique d’une pommade antimicrobienne à base d’un extrait hydroalcoolique de *Bersama abyssinica* Fresen. *Ethnopharmacologia*, n°58, 2017.

Treated Olive Husk flour in a PVC-Based Composite Material: Recycling Effect on Physico-Mechanical and Rheological Properties

Lisa Klaai*, Dalila Hammiche; Hassina Aouat; Amar Boukerrou

Laboratoire des Matériaux Polymères Avancés (LMPA), Faculté de Technologie, Université de Bejaia, 06000 Bejaia, Algérie

Corresponding author* lisa.klaai@univ-bejaia.dz

Received: 04 January 2022; Accepted: 24 January 2022; Published: 29 January 2022

Abstract

The work is directed to study the recycling effects on the olive husk flour reinforced polyvinylchloride composites with and without maleic anhydride-grafted polyvinyl chloride used as compatibilizer. To improve the fiber-matrix adhesion, olive husk flour was chemically treated by benzoylation treatment. The material was characterized after each extrusion using tensile tests, Rheological measurements, scanning electron microscopy (SEM), and Size Exclusion Chromatography (SEC). Results indicated that generally after four cycles, the recycled composites had considerably higher modulus as compared with the original composites which were attributed to changes in physical and chemical properties of the composites induced by the recycling process. This effect was enhanced for the compatibilized samples. Increase of the modulus strength of the poly (vinyl chloride) (PVC) matrix is detected due to the molecular chain cross-linking resulting from degradation.

Keywords: Poly (vinyl chloride), Benzoylation treatment, Olive Husk flour, Recycling, Physico-Mechanical properties.

I. Introduction

In recent decades, the increase in world population and the need to adopt better living conditions have led to a dramatic increase in the consumption of polymers, mainly plastics, resulting in the generation of waste in large quantities. To reduce the environmental problems caused by the accumulation of this waste, it is in our interest to recycle it [1].

Several research works have focused on the effect of recycling on composites based on polypropylene, polyethylene and vegetable fibres [2]

Petchwattam et al [3] carried out a study on the recycling of composites based on polyvinyl chloride and wood flour (WF), their work is composed of two parts, the first focuses on the recycling of the mixture of industrial waste from PVC/WF composites and PVC pellets reinforced with WF. The second part consists in recycling the PVC/WF composites (seven extrusion cycles), according to their results they found that the recycling reduced the molecular weight of the PVC matrix, they explained this reduction by the scission of chains molecule by shear stress during the recycling process. On the other hand, the results of

the mechanical tests have shown that PVC/WF composites can be recycled again as composites without critically affecting their mechanical performance.

Hammiche et al [4] studied the effect of mechanical recycling on the properties of PVC/Alfa composites. They prepared three formulations, Virgin PVC, Composite loaded with 20% of alfa in the presence and in the absence of 5% of PVC-g-MA.

The composites produced underwent four extrusion cycles. According to their results, they found that the mechanical properties of composites increase with the number of recycling cycles. Indeed, the tensile strength and the Young's modulus in the studied formulations increased considerably. These are clearly revealed by scanning electron microscopy (SEM). After recycling, the morphology of the composite materials indicates that the alfa fiber particles are uniformly dispersed and embedded in the polymer matrix. They also observed that the maximum degradation rate is shifted to a slightly higher region in the case of composites compared to virgin PVC, due to the higher thermal stability of composites.

This work is devoted to the study of the effect of mechanical recycling on the properties of PVC/Olive husk flour composites. Four formulations were prepared, virgin PVC, the composite loaded with 20% untreated olive husk flour and treated by benzylation and also the composite loaded with 20% olive husk flour in the presence of 5% PVC-g-MA.

A series of four extrusion cycles was carried out on the four formulations using an internal mixer equipped with two counter-rotating screws.

II. Material and methods

Provide sufficient detail to allow the work to be reproduced. Methods already published should be indicated by a reference: only relevant modifications should be described.

II.1 Material

The used Polyvinyl chloride (PVC), type SE-1200, has K-Wert value of 70.20 to 72.00, viscosity value of 0.99-1.030 and a density of 0.481-0.561

The main additives of PVC were summarized in table 1.

Table 1: Additives of PVC SE-1200

Additives	Names	Value (%)
Plasticizer	Diocetyl Phthalate (DOP)	30
Stabilizer	Ca/Zn	4
Lubricant	Stearic Acid	0.5

The filler used was olive husk flour; it was obtained after olives processing for oil in the region of Bejaia (Algeria). The olive husk has sustained several pre-treatments, namely washing with hot water to eliminate pulp, drying under ambient conditions for 48 h, grinding, and sieving to have a grain size of $\leq 100 \mu\text{m}$ [5].

The reagents used for benzylation of olive husk flour are sodium hydroxide (MW=40) and benzoyl chloride (MW=140.56) which are supplied by BIOCHEN CHERMOPHARMA.

PVC-g-MA was synthesized at the laboratory of organic materials A. Mira University of Bejaia, Algeria by Hammiche et al [6]. The addition of a coupling agent aims for interfacial adhesion improvement.

II.2 Methods

Chemical modification of olive husk flour by benzylation

This modification was carried out according to the following experimental protocol: 35g of olive husk

flour were soaked in an 18% NaOH solution for 30min, followed by filtration and washing with distilled water. The treated flour was then suspended in a 10% NaOH solution with 50ml of benzoyl chloride with stirring for 15min, the contents are kept at room temperature for 15min, then the mixture was filtered, washed and dried at room temperature, the isolated flour was then soaked in ethanol (96%) for one hour to remove excess benzoyl chloride and finally, the mixture was filtered, washed and dried in an oven at 60°C for 24 hours.

Preparation of composites

To study the effect of recycling on composite materials, composites were prepared in two steps. The first step consists of mixing the different constituents in an internal mixer. The second is to grind them then mold them by compression at 180°C with a pressure of 30bar to obtain films with an average thickness of 150 μm . The same processed samples are recycled four times in the internal mixer. These are characterized after each transformation cycle.

The mixtures are made using a Brabender type mixer, Plasticorder W 50 EHT. The PVC-g-MA compatibilizers and the olive husk flour treated and untreated are first steamed at 60°C for 24 hours. The various constituents are mixed manually then introduced into the Brabender for 5 min, at a temperature of 180° C. and a rotation speed of 50 rpm.

Mass compositions of the various formulations are given in Table 2.

Table 2: Mass composition of the different formulations

	PVC compound (%)	OHF (%)	OHFT (%)	PVC-g-MA (%)
PVC	100	0	0	0
PVC/OHF	80	20	0	0
PVC/OHFT	80	0	20	0
PVC/PVC-g-MA/OHF	75	20	0	5

Tensile test

The tensile tests of formulations PVC, PVC/OHF, PVC/OHFT and PVC/PVC-g-MA/OHF composites were carried out on an MTS synergy RT1000 type tensile machine at ambient temperature (23° C.) and a displacement speed of 2 mm/min. in this study, the results presented are the average of five trials for each sample.

Rheological measurements

The rheological behavior of virgin PVC and composites obtained was studied in dynamic mode using a dynamic rotational shear rheometer (Rheometer AntonPaar MCR 301). The jaws are of plane/plane geometry with a diameter of 25mm in oscillatory mode at 175°C, which makes it possible to evaluate the viscoelastic properties such as the storage and loss moduli, and the complex viscosity. The strain imposed is 2%. It is determined so as to remain in the linear domain during the amplitude sweep. The samples were prepared by compression in a mold at 180°C in the form of a disc approximately 1.5mm thick. The elastic modulus and the complex viscosity have been measured in the linear domain, for frequencies ranging from 100 to 0.01Hz.

Morphological characterization

The morphological analysis of virgin PVC and composites was carried out using a brand name scanning electron microscope (SEM) (Joel JSM 6460LV). The samples to be analyzed were prepared by fracturing after immersing them in liquid nitrogen.

Size Exclusion Chromatography (SEC)

The analysis was carried out by a device of the shimadzu RID 10 A type. The sample to be analyzed is dissolved in tetrahydrofuran, the samples are put in solution with stirring for 12 hours, and before injection the solutions are filtered on a dynaguard filter of porosity 0.20 μm.

III. Results and discussion

Tensile test

Mechanical property is a characteristic property of a material that describes its behavior when subjected to one or more mechanical stresses, the most common measures are: Young's modulus, tensile strength and elongation at break. Figure 1 illustrates the evolution of tensile strength, Young's modulus and elongation at break as a function of the number of transformation cycles of the polyvinyl chloride matrix, treated and untreated PVC/OHF composites and PVC/PVC-g-MA/OHF. In the first processing cycle, a significant increase in Young's modulus is recorded with the addition of flour. However, this increase is more remarkable in the presence of PVC-g-MA. On the other hand, we observed a decrease in the tensile strength of the composites compared to virgin PVC.

The increase in the strength of virgin PVC is less marked with recycling, there is a slight decrease in

strength in the first cycle then an increase in this property in the fourth cycle, and this is probably due to the crosslinking of PVC induced by the artwork.

The increase in strength at break of PVC/OHF, PVC/OHFT and PVC/PVC-g-MA/OHF composites is recorded, going from 5.4MPa, 9.1MPa, and 9.4MPa, respectively in the first cycle to 9MPa, 13.6MPa and 12.1MPa and this is due to better flour dispersion in the matrix due to the reduction in melt viscosity [7].

contrary to virgin PVC, the Young's modulus of the composites show a strong increase induced not only by the reduction in the dimension of the flours caused by the grinding but also by their good dispersion and therefore an improvement in the interfacial adhesion between the matrix and the reinforcement especially in the presence of PVC-g-MA and at the third cycle of transformation.

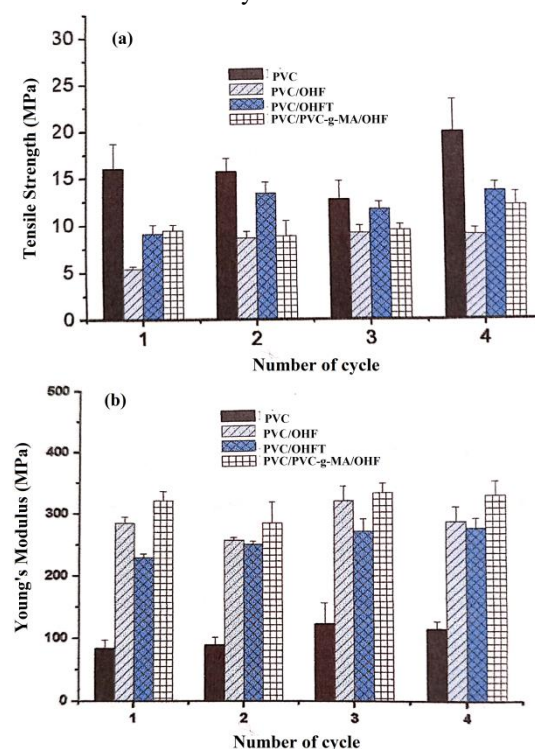


Figure 1: Evolution of (a) tensile strength and (b) Young's modulus as a function of the number of transformation cycles of the polyvinyl chloride matrix, treated and untreated PVC/OHF composites and PVC/PVC-g-MA/OHF

Pillin et al [8] conducted a study on the effects of extrusion cycles on the mechanical properties of polylactic acid (PLA). They found that the number of extrusion cycles has no influence on the tensile modulus; they assumed that this value remains constant because the potential decrease in the molecular weight of PLA is compensated by an increase in its crystallinity. On the other hand, the

recycling effect on the tensile strength of PLA is very significant, leading to a great reduction in this characteristic; it goes from 66 MPa to 25 MPa after 7 cycles. This strong decrease is attributed to a lower cohesion in the material, probably due to a decrease in the molecular pods and therefore the resistance of the entanglement between the chains. They also observed the decrease in the strain at break from 6% to 0.8%. This phenomenon may be a consequence of both the decrease in chain length and the increase in the degree of crystallinity, both of which favour the propagation of cracks above the elastic domain. Similarly Kaci et al [9] have carried out a study on the effects of repeated extrusion cycles on the structure and properties of PP/wood flour composites in the presence and absence of the terpolymer of butyl acrylate glycidyl ethylene methacrylate (EBAGMA) used as a compatibilizer agent. They compared the variation of the modulus according to the number of cycles of the composites PP/WF, PP/WF/EBAGMA and virgin PP. They found that the tensile modulus for virgin PP is about 1270MPa and this value increases by about 15% in compatible PP/WF composite materials. They attributed this increase to the effect of the grafting of the EBAGMA terpolymer on the PP chains. They also observed that the tensile modulus for composite materials is not affected by repeated extrusion cycles. On the other hand, the effect of reprocessing on the tensile modulus of PP is drastic causing a strong reduction in this characteristic of about 40% between the second and the third cycle. This is probably due to the decrease in molecular weight, due to the phenomenon of chain scission, induced by recycling. They also observed that the tensile strength of virgin PP is around 34MPa. On the other hand, the increase in the number of transformation cycles induces a significant drop in the breaking stress of virgin PP to reach 9 MPa after the third cycle. The addition of 20% by weight of WF to the polymer leads to a reduction in the initial value of the breaking stress to about 20 MPa due to the poor interfacial adhesion between the matrix and the flour. When the compatibilizer is added to the PP/WF composites, the breaking stress is slightly increased from 20 to 24MPa. This improvement is generally attributed to better interfacial adhesion and the reinforcing effect of the flour. Both for the non-compatible composite samples and those compatible with EBAGMA, they

observed a very slight decrease in the breaking stress (about 5%).

The recycling process which can induce the decrease in molecular weight in the polymer matrix does not significantly affect in the mechanical properties of the composites.

It is observed that the elongation at break (Figure 2) of the PVC matrix is less affected by recycling; it is around 208% in the first transformation cycle and 198% in the fourth transformation cycle. The addition of olive husk flour to the PVC matrix significantly reduces the elongation at break and this is due to the rigidity induced by the vegetable flour. Generally, the addition of the lignocellulosic filler causes a significant reduction in the ductility of the composite [10]. Recycling causes a decrease in this elongation until the third transformation cycle probably caused by the good dispersion of the flour in the polymer matrix as well as better adhesion between the two constituents, causing a decrease in elongation especially in the presence of PVC-g-MA. According to Bourmaud et al [11], the increase in the fracture strain of the composite is attributed to the loosening of the reinforcement particles from the matrix due to their poor adhesion. Hamad et al [12] have found that the elongation at break of the poly (lactic acid)/polystyrene mixture decreases by a factor of 0.61 after two processing cycles and by a factor of 0.73 after four processing cycles. This phenomenon may be a consequence of both the reduction in the molecular chain length and the increase in the degree of crystallinity, which both favour the propagation of cracks above the elastic domain.

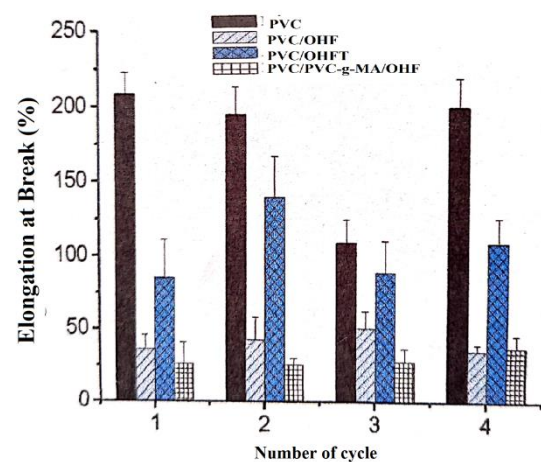


Figure 2: Evolution of elongation at break as a function of the number of transformation cycles of the polyvinyl chloride matrix, treated and untreated PVC/OHF composites and PVC/PVC-g-MA/OHF

Rheological measurements

The rheological measurements are carried out with the aim of evaluating the effect of the number of transformation cycles on the viscoelastic properties and on the state of dispersion of the flour.

Figures 3 and 4 show the evolution of the elastic modulus as a function of the formation of the PVC, PCV/OHF, PVC/OHFT, and PVC/PVC-g-MA/OHF formulations after recycling, carried out at a frequency of 1Hz at 180°C.

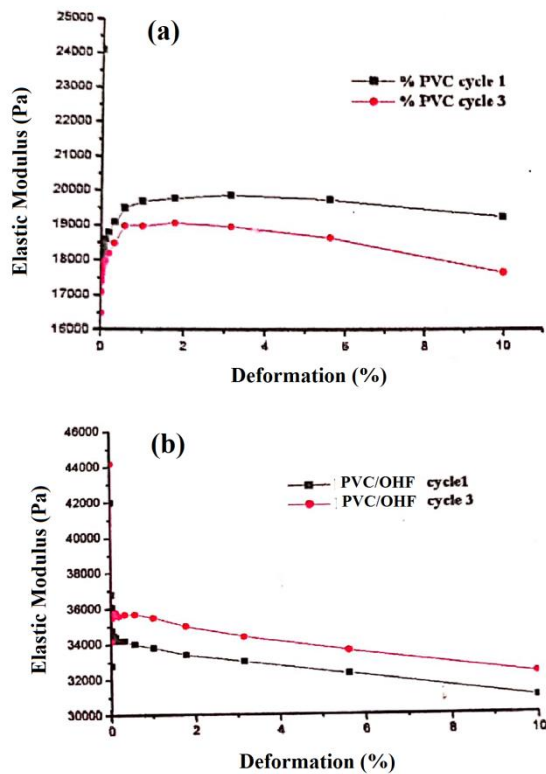


Figure 3: Evolution of the elastic modulus as a function of the formation of the PVC and PCV/OHF formulations after recycling

The linear viscoelastic domain extends only at a strain of 0.5%. The linear viscoelastic properties are therefore determined for all the formulations at this strain of 0.5%. It is observed that the addition of flour causes a reduction in the linear viscoelasticity range of the composites. The network structure comes from the entanglements present in the amorphous phase as well as from the order characterizing the semi-crystalline phase of PVC. This network structure maintains a large deformation, but in the composite a new microstructure is formed. This does not resist large deformation compared to the virgin matrix.

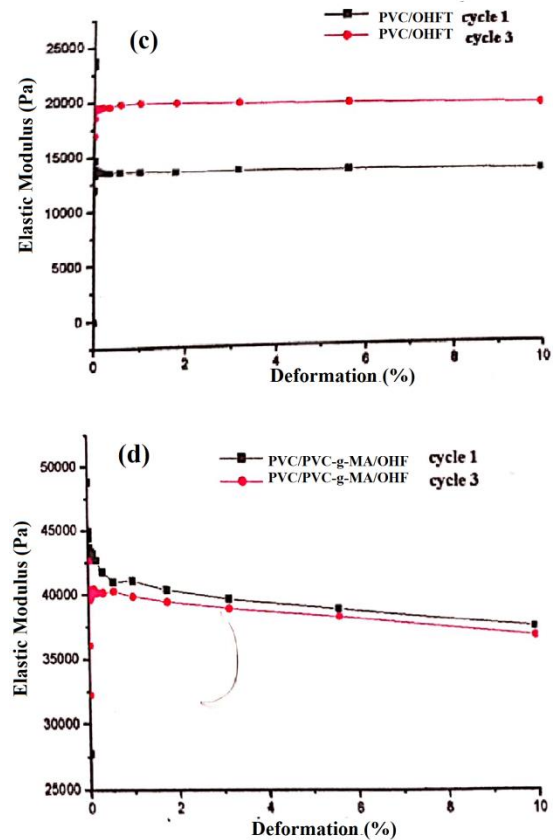


Figure 4: Evolution of the elastic modulus as a function of the formation of PVC/OHFT and PVC/PVC-g-MA/OHF formulations after recycling

Figures 5 and 6 present the evolution of the elastic, viscous modulus and the complex viscosity as a function of the frequency of the PVC matrix and the composites in the 1st and 3rd transformation cycle. Polyvinyl chloride show a mainly viscous elastic behavior, it can be concluded that PVC behaves as a homogeneous melt only above a critical temperature while below this temperature it exhibits rheological characteristics unknown to others, molten polymers but typical for cross-linked polymer systems [13].

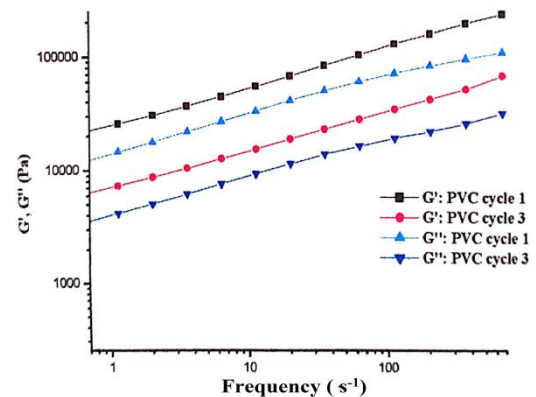


Figure 5: Evolution of the elastic, viscous modulus as a function of the frequency of the PVC matrix in the 1st and 3rd transformation cycle.

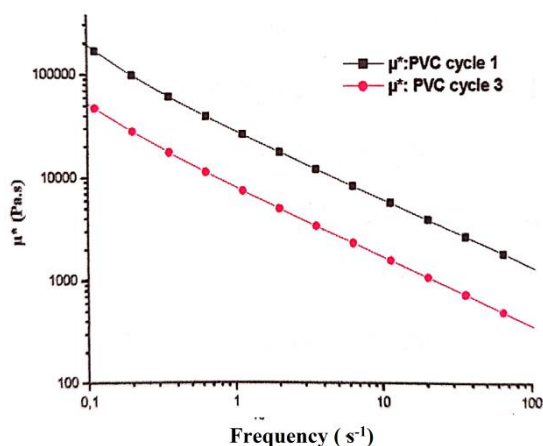


Figure 6: Evolution of complex viscosity as a function of the frequency of the PVC matrix in the 1st and 3rd transformation cycle.

After recycling, a decrease in the elastic and viscous modulus and in the complex viscosity of the PVC is recorded. The viscosity of polymers depends on both the weight average molar mass M_w and the molar mass distribution of the material. The decrease in the complex viscosity is therefore linked to the decrease in the average molecular mass in weight M_w due to the chain scission reactions. According to Gonzalez et al [14] this occurs in the case of thermomechanical aging of polyvinyl chloride on the chains with the highest molecular masses and preferentially in the centre of the macromolecules.

Figure 7 represents the evolution of the complex viscosity as a function of the frequency of the composites between the 1st and the 3rd transformation cycles. According to the results, an increase in the complex viscosity of the untreated PVC/OHF and PVC/OHF composites is observed in the presence of the compatibilizer agent PVC-g-MA after recycling. This is interpreted as the result of a strong interaction between the matrix indicating an improvement in the state of dispersion [15].

However, for flour composites treated by benzoylation, a decrease in viscosity is recorded, and this can be attributed to chain scission which leads to a reduction in molecular weight [16].

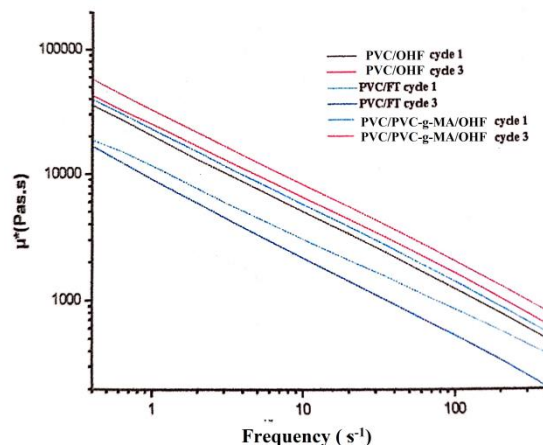


Figure 7: Evolution of the complex viscosity as a function of the frequency of the composites between the 1st and the 3th transformation cycles.

Size Exclusion Chromatography (SEC)

The average molecular weights M_w and the molecular weight distributions (polydispersity index) I_p of PVC and the composites with and without PVC-g-MA at the first and third processing cycle are shown in Figure 8 and 9, respectively. It turns out that the masses molecular weight increases after mechanical recycling. An increase in the polydispersity index is also observed. Indeed, after four cycles we can observe an increase in M_w . The degradation of the polymer matrix is accelerated especially in the presence of olive husk flour leading to dehydrochlorination, formation of unsaturation and then crosslinking of the chains of our materials. Consequently, the length of the molecular chains of the polymer increases and the matrix shows better mechanical properties which in turn increase the mechanical properties of the composite [17] leading to dehydrochlorination, formation of unsaturation and then crosslinking of the chains.

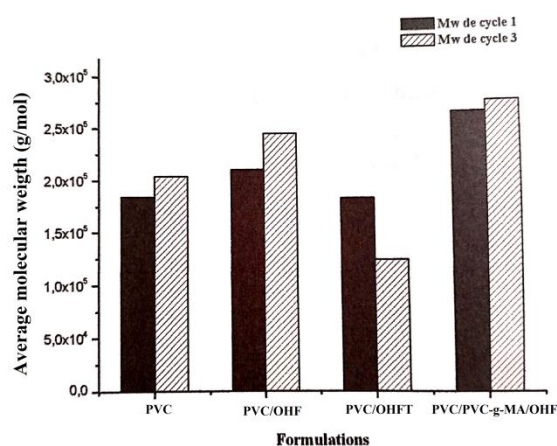


Figure 8: Average molecular weights Mw of PVC and the composites with and without PVC-g-MA at the 1st and 3rd processing cycle

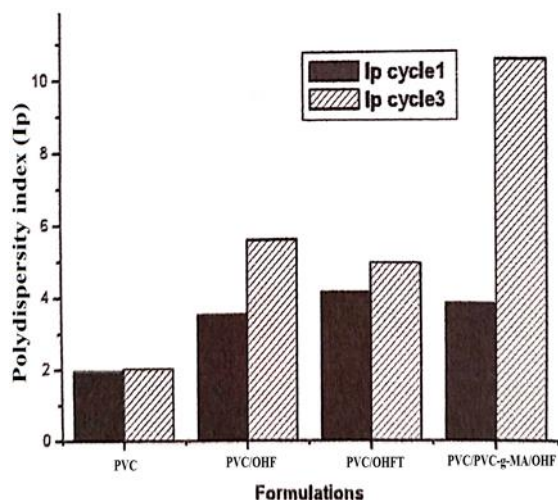


Figure9: molecular weight distributions (polydispersity index) Ip of PVC and the composites with and without PVC-g-MA at the 1st and 3rd processing cycle

Morphological characterization

Figure 8 represents the pictures obtained by SEM of the PVC/OHF, PVC/OHFT, and PVC/PVC-g-MA/OHF composites at 1st cycle and at the 3rd transformation cycle. The results of the first cycle (figure 10 (a)) reveal that the flour is completely stripped from the matrix, which shows that the adhesion is very weak between the matrix and the untreated olive husk flour, the benzoylation and the coupling improve the adhesion between the PVC and OHF, we observe the decrease in the number and the size of the cavities for the composites treated by benzoylation (figure 10 (c)) [18]. In the fourth transformation cycle, we notice the reduction in diameter of the flours compared to the first cycle, confirming the fibrillation. This also explains the increase in the modulus of recycled composites caused by the decrease in the form factor after recycling [19].

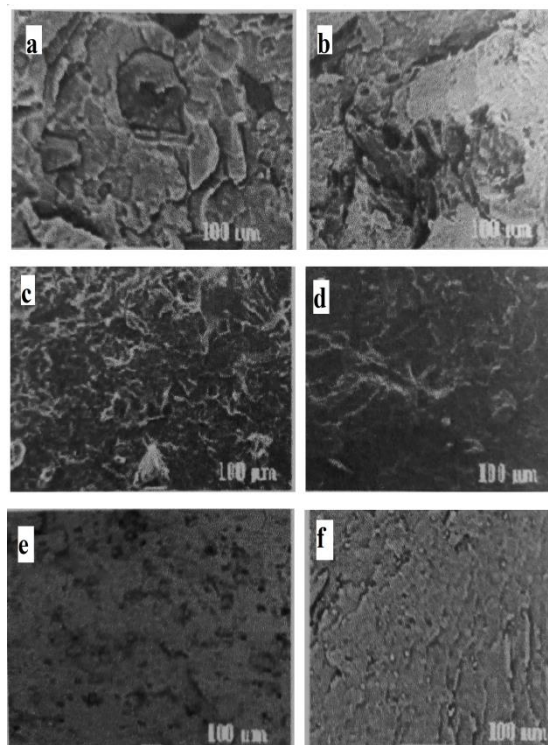


Figure 10: pictures obtained by SEM of the PVC/OHF, PVC/OHFT, and PVC/PVC-g-MA/OHF composites at the 1st cycle and at the 3rd transformation cycle

IV. Conclusions

In conclusion, the aim of this work is to study the mechanical and rheological properties of PVC/OHF composites treated and untreated by benzoylation and with the coupling agent PVC-g-MA as a function of the mechanical recycling number. The results showed that generally the mechanical properties of the composites increase with the number of recycling. Indeed, the tensile strength and the Young's modulus in the studied formulations increased considerably. Recycling has caused chain scissions which are manifested by a decrease in viscoelastic properties for flour composites treated by benzoylation.

Conflict of interest

The authors declare that they have no conflict for financial interests or personal relationships that how can influence the work reported in this paper.

References:

- [1] K. Hamad, M. Kaseem, F. Deri. Recycling of waste from polymer materials: An overview of the recent works. *Polymer Degradation and Stability*, 98, 2801-2812, 2013

- [2] A. Ashori, S. Sheshmani. Hybrid composites made from recycled materials: Moisture absorption and thickness swelling behavior. *Bioresource Technology*, 101, 4717-4720, 2010
- [3] N. Petchwattana, S. Covavisaruch, J. Sanetuntikul. Recycling of wood-plastic composites prepared from poly(vinyl chloride) and wood flour. *Construction and Building Materials*, 28, 557-560, 2012
- [4] D. Hammiche, A. Bourmaud, A. Boukerrou, H. Djidjelli, Y. Grohens. Number of processing cycle effect on the properties of the composites based on alfa fiber. *Journal of Thermoplastic Composite Materials*, 29, 1176-1193, 2016
- [5] H. Aouat, D. Hammiche, A. Boukerrou, H. Djidjelli, Y. Grohens, I. Pillin. Effects of interface modification on composites based on olive husk flour. *Materials Today: Proceedings* 36, 94-100, 2021
- [6] D. Hammiche, A. Boukerrou, H. Djidjelli, M. Beztout, S. Krim. Synthesis of a new compatibilisant agent PVC-g-MA and its use in the PVC/alfa composites. *Journal of Applied Polymer Science* 124, 4352-4361, 2012
- [7] G. Guerrica-Echevarría, J. Eguiazábal, J. Nazábal. Effects of reprocessing conditions on the properties of unfilled and talc-filled polypropylene. *Polymer Degradation and Stability*, 53, 1-8, 1996.
- [8] I. Pillin, N. Montrelay, A. Bourmaud, Y. Grohens. Effect of thermo-mechanical cycles on the physico-chemical properties of poly(lactic acid). *Polymer Degradation and Stability*, 93, 321-328, 2008
- [9] M. Kaci, A. Hamma, I. Pillin, Y. Grohens. Effect of Reprocessing Cycles on the Morphology and Properties of Poly(propylene)/Wood Flour Composites Compatibilized with EBAGMA Terpolymer. *Macromolecular Materials and Engineering*, 294, 532-540, 2009.
- [10] M. Islam, M. Rahman, M. Haque, M. Huque. Physico-mechanical properties of chemically treated coir reinforced polypropylene composites. *Composites Part A-applied Science and Manufacturing*, 41, 192-198, 2010
- [11] A. Bourmaud, C. Baley. Investigations on the recycling of hemp and sisal fibre reinforced polypropylene composites. *Polymer Degradation and Stability*, 92, 1034-1045, 2007
- [12] K. Hamad, M. Kaseem, F. Deri. Effect of recycling on rheological and mechanical properties of poly (lactic acid)/polystyrene polymer blend. *Journal of Materials Science*, 46, 3013-3019, 2011
- [13] H. Müunstedt. Relationship between rheological properties and structure of poly(vinyl chloride). *Journal of Macromolecular Science, Part B, Physics*, 14, 195-212, 1977
- [14] V.A.G. González, G.N. Velázquez, J.L.A. Sánchez. Polypropylene chain scissions and molecular weight changes in multiple extrusion. *Polymer degradation and stability*, 60(1), 33-42, 1998
- [15] J.K. Mishra, K.J. Hwang, C.S. Ha. Preparation, mechanical and rheological properties of a thermoplastic polyolefin (TPO)/organoclay nanocomposite with reference to the effect of maleic anhydride modified polypropylene as a compatibilizer. *Polymer*, 46(6), 1995-2002, 2005
- [16] L. Delva, K. Ragaert, J. Degrieck, L. Cardon. The effect of multiple extrusions on the properties of montmorillonite filled polypropylene. *Polymers*, 6(12), 2912-2927, 2014
- [17] M.P. Foulc, A. Bergeret, L. Ferry, P. Ienny, A. Crespy. Study of hygrothermal ageing of glass fibre reinforced PET composites. *Polymer Degradation and Stability*, 2005, 89 (3), 461-470, 2005
- [18] L. Augier, G. Sperone, C. Vaca-Garcia, M.E. Borredon. Influence of the wood fibre filler on the internal recycling of poly (vinyl chloride)-based composites. *Polymer Degradation and Stability*, 92(7), 1169-1176, 2007
- [19] M.S. Ramle, A.Z. Romli, M.H. Abidin. Tensile properties of aminosilane treated rice husk/recycled PVC composite. *Advanced Materials Research*, 812, 151-156, 2013

Analytical and numerical investigation of displacements and stresses in thick-walled FGM cylinder with exponentially-varying properties

Chahinaz Medjane¹; Abdelhakim Benslimane^{2*}; Nadir Mesrati¹

¹ *Departement of Metallurgy, National Polytechnic school of Algiers, 16000 Alger, Algérie.*

² *Laboratoire de Mécanique Matériaux et Énergétique (L2ME), Faculté de Technologie, Université de Bejaia, 06000 Bejaia, Algérie.*

*Corresponding author email: abdelhakim.benslimane@univ-bejaia.dz

Received: 09 January 2022; Accepted: 29 January 2022; Published: 29 January 2023

Abstract

In this paper, analytical solutions are presented for computing mechanical displacements and stresses in a thick-walled cylindrical made of functionally graded materials (FGMs) under mechanical loading. The pressure vessel is subject to axisymmetric internal pressure. The analytical model of the pressurized vessel is constructed, where the radial continuous varying of elastic modulus along the thickness was assumed. It has been assumed that the elastic modulus is varying through thickness of the FGM material according to an exponential distribution along the thickness. Navier's equation, which is a second-order ordinary differential equation, was derived from the mechanical equilibrium equation. The distributions of the displacement and stresses were determined by the exact solution to Navier's equation. The effect of the inhomogeneity parameter and internal pressure on radial displacement, radial, tangential and axial stresses in a functionally graded cylinder is analyzed. Results obtained clarify the influence of the mechanical field, non-homogeneity parameter on the elastic response of the functionally graded cylindrical vessel. This is depicted graphically by using radial displacement and stresses in a pressurized functionally graded cylinder. Thus, these parameters have remarkable effects on the distributions of radial displacement and radial and circumferential stresses. The inhomogeneity constant, which includes continuously varying volume fraction of the constituents, is a useful parameter from a design point of view in that it can be tailored for specific applications to control the stress distribution.

Keywords: Stresses, elasticity, FGM, Thick cylinders, mechanics, exponential distribution.

I. Introduction

Functionally graded materials (FGMs) are the advanced form of composite materials. The main advantage of using FGM over composite material is that it provides the freedom of continuous and directional gradation of specific properties on a macroscopic level, which eliminates the effect of interlaminar stresses and leads to increase in the overall performance of component [1]. FGM structures are most commonly used in civil structures, mechanical structures like, helicopter rotor blades, robot arms, turbine blades and space erectable booms, etc. [2-3]

Thick-walled cylindrical vessels and hollow cylinders are commonly used components in different structural applications and device systems in many industries involving aerospace and submarine structures, civil engineering, mechanical engineering, pipes, sensors and actuators, etc. [4-7]. Until recently, these cylindrical objects are made of isotropic homogeneous materials which can only be optimized for their applications by material selection and

very limited dimensional design. In recent decades, functionally graded materials have become widespread due to possibility they offer for optimization of the design in terms of the spatial distribution of material properties.

Within the framework of theory of elasticity, the analysis of such hollow structures subjected to internal and/or external pressures and temperature may be of great interest regarding the importance of design in solid mechanics.

FG Materials are microscopically non homogeneous but at macro level, the mechanical properties vary continuously from one surface to another by smoothly varying the volume fractions of the material constituents [8,9]. Obviously FGM could be used in a variety of applications which have made them very attractive. In addition to their good thermal properties, they are corrosion and erosion resistant and have high fracture resistance [10, 11]. FGM are fabricated by continuously changing the volume fraction of two basic materials, usually ceramic and metal, in one or more directions. The FGM that are thus formed exhibit isotropic yet non-homogenous thermal and mechanical properties.

These kinds of materials are treated as non-homogenous with material contents that vary continuously along one spatial direction.

Analytical solutions for the elastic behaviors of cylinders were provided by Tutuncu and Ozturk [12], Sburlati [09], Nejad and Fatehi [13], among others. Nejad and Fatehi [13] proposed an exact solution of an elastoplastic rotating thick-walled cylindrical pressure containers built of functionally graded materials. Chen and Lin [14] used the transmission matrix approach to statistically evaluate the elastic behavior of thick-walled, single or multi-layered, and arbitrarily graded cylinders/spheres. Nie et al. [15] presented a method for tailoring materials that are graded by a radially varying volume fraction rule to achieve through-the-thickness either a constant circumferential stress or a constant in-plane shear stress. This method is applicable to linear elastic hollow cylinders and spheres. Nie and Batra [16] employ the Airy stress function to derive analytical solutions for plane strain static deformations of a functionally graded (FG) hollow circular cylinder with Young's modulus E and Poisson's ratio ν taken to be functions of the radius r . Besides assuming that the material properties vary according to a power-law function of r , some investigators have presumed that the elastic moduli is exponential functions of r . Based on the assumption that Poisson's ratio ν is constant and Young's modulus E is an exponential function of r [17–19], have analyzed stresses and displacements in FG cylindrical pressure vessels. Existing analytical solution for elastic field in pipes are available when Young's modulus is expressed by the power law expression [20–22]. Ghannad and Gharooni [23] employed the first-order shear deformation theory to analyze the elastic characteristics of pressured thick FGM cylinders with exponential variation. A numerical elastic study was performed by Chen and Lin [24] for a thick cylinder or sphere constructed of exponentially graded materials. Dai et al. [25] reviewed most of the researches in years (2005–2015) on FGM cylindrical structures.

Existing analytical solution for elastic field in pipes are available when Young's modulus is expressed by the power law expression. For the exponential law, the most existing solutions in the literature are numerical. In order to fill this gap, an exponential function form for the spatial variation of the stiffness proposed was used in this work. We study the distribution of stresses in a thick wall of a cylinder in FGM under internal pressure. The equilibrium equation is transformed into a nonlinear differential equation that we have solved analytically.

However, designing of a cylinders made of FGM requires understanding and quantifying the elastic field in these elements. In an attempt to achieve this goal, this study concentrates on the analysis of elastic field in a cylinder FGM subjected to internally and/or externally pressurized.

In this paper, using the elasticity solution, the elastic behavior of the functionally graded thick-walled tube subjected to axisymmetric mechanical load is investigated in this work. In Section 2 the basic equations of the FGM long tube and the analysis of mechanical behaviors of the tube are described. Section 3 gives the results and discusses the obtained results.

II. Problem formulation

We consider a hollow FGM cylinder. The cylinder has inner and outer radii, respectively, R_{in} and R_{out} . It is subjected to mechanical loading. The materials are assumed linearly elastic and isotropic and the graded materials Young's modulus depend only on the radial direction while Poisson's ratio is assumed constant. The schematization of the thick tube is shown in Fig. 1.

For convenience, the axisymmetric load conditions require considering a cylindrical coordinate system (r, θ, z) .

To ascertain the effect of the inhomogeneity, expression of Young's modulus is considered across the thickness:

$$E(r) = E_i e^{\left(\frac{\alpha(r-R_i)}{R_o-R_i}\right)} \quad (1)$$

Where $E(r)$ is Young's modulus. E_i is the values of Young's modulus at $r = R_{in}$. α is the parameter of the inhomogeneity material. Homogenous case is obtained when $\alpha = 0$.

Let \mathbf{u} be the displacement field, where $u_i (i = r, \theta, z)$ are the components of displacement, respectively. The length of the cylinder is sufficiently large so that we confine our attention to the plain strain problem.

In the case of plane elasticity, the displacement, stress and strain fields may be written:

$$\mathbf{u} = \mathbf{u}(r), \quad \sigma_{ij} = \sigma_{ij}(r), \quad \varepsilon_{ij} = \varepsilon_{ij}(r) \quad (2a,b,c)$$

The cylinder's material is graded through the r -direction, thus the material properties are functions of r . Let u_r be the displacement component in the radial direction and since the elastic field is axisymmetric and independent of z , the kinematic relations (strain-displacement) are given:

$$\varepsilon_{rr} = \frac{\partial u_r}{\partial r}, \quad \varepsilon_{\theta\theta} = \frac{u_r}{r}, \quad \varepsilon_{zz} = \varepsilon_{rz} = \varepsilon_{r\theta} = \varepsilon_{\theta z} = 0 \quad (3a,b,c)$$

The cylinder is made of elastic inhomogeneous material which is described by Hooke's law which is given by :

$$\sigma_{ij} = 2\mu(r)\varepsilon_{ij} + \lambda(r)\varepsilon_{ii}\delta_{ij} \quad (4)$$

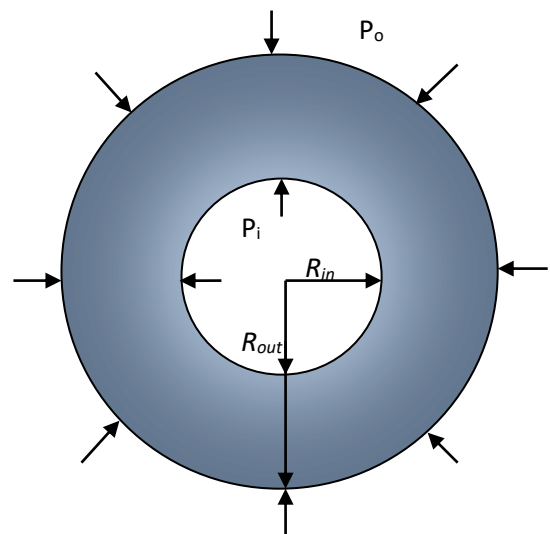


Figure 1. Thick circular cylinder with wall in FGM.

where: $\mu(r) = \frac{E(r)}{2(1+\nu)}$ and $\lambda(r) = \frac{\nu E(r)}{(1+\nu)(1-2\nu)}$ are Lamé's constants, $E(r)$ is Young's modulus which depends on spatial coordinates and ν the Poisson's ratio.

The stress-strain relations in elastic steady state problem are given:

$$\begin{cases} \sigma_{rr} = (2\mu(r) + \lambda(r)) \cdot \varepsilon_{rr} + \lambda(r) \cdot \varepsilon_{\theta\theta} \\ \sigma_{\theta\theta} = (2\mu(r) + \lambda(r)) \cdot \varepsilon_{\theta\theta} + \lambda(r) \cdot \varepsilon_{rr} \\ \sigma_{zz} = \lambda(r)(\varepsilon_{rr} + \varepsilon_{\theta\theta}) \end{cases} \quad (5)$$

where σ_{rr} , $\sigma_{\theta\theta}$ and σ_{zz} are the radial, circumferential and axial components of the Cauchy stress tensor.

III. Analytical solution

The equilibrium equation for a cylindrical vessel in an axisymmetric problem, disregarding the body forces and the inertia terms, is written in cylindrical coordinates as follows:

$$\frac{\partial \sigma_{rr}}{\partial r} + \frac{\sigma_{rr} - \sigma_{\theta\theta}}{r} = 0 \quad (6)$$

To obtain the equilibrium equation in terms of the displacement component for the cylinder made of FG Material, the functional relationship of the material properties must be known.

For convenience, we assume:

$$\begin{aligned} \lambda(r) &= \psi(\nu) \cdot E(r), 2\mu(r) + \lambda(r) = \zeta(\nu) E(r) \\ \psi(\nu) &= \frac{\nu}{(1+\nu)(1-2\nu)}, \zeta(\nu) = \frac{(1-\nu)}{(1+\nu)(1-2\nu)} \end{aligned} \quad (7)$$

Substituting the kinematic relations in Eq. (3) into Hooke's law in Eq. (4) and then into the equations of equilibrium Eq. (6) gives the following differential equation governing the radial displacement field:

$$r^2 \frac{d^2 u}{dr^2} + (Ar+1)r \frac{du}{dr} - \left(1 - \frac{\psi(\nu)}{\zeta(\nu)} Ar\right) u = 0 \quad (8)$$

where: $A = \frac{dE(r)}{E(r)dr}$

Substituting Eqs. (1) in Eq. (8) then we obtain the following form of the differential equation:

$$\begin{aligned} r^2 \frac{d^2 u}{dr^2} + \left(\frac{\alpha}{R_{out} - R_{in}} r + 1 \right) r \frac{du}{dr} \\ - \left(1 - \frac{\psi(\nu)}{\zeta(\nu)} \frac{\alpha}{R_{out} - R_{in}} r \right) u = 0 \end{aligned} \quad (9)$$

The solution for the differential equation (9) can be expressed:

$$\begin{aligned} u(r) &= Ar^{\frac{1}{2}} e^{\left(\frac{\alpha r}{2(R_{in} - R_{out})}\right)} M\left(a_1, b_1, \frac{\alpha r}{(R_{in} - R_{out})}\right) \\ &+ Br^{\frac{1}{2}} e^{\left(\frac{\alpha r}{2(R_{in} - R_{out})}\right)} W\left(a_1, b_1, \frac{\alpha r}{(R_{in} - R_{out})}\right) \end{aligned} \quad (10)$$

With: $a_1 = \frac{3\nu-1}{2\nu-2}$, $b_1 = 1$

The basic properties of Kummer's function can be found in various mathematical references (Abramowitz and Stegun [26]) and they are available in many computer programs.

In the case of a cylinder subjected to internal and external pressures respectively, P_i and P_o , the constants A and B can be obtained from the following boundary conditions:

$$\begin{cases} \sigma_{rr}|_{r=R_{in}} = -P_i \\ \sigma_{rr}|_{r=R_{out}} = -P_o \end{cases} \quad (11)$$

IV. Results and discussion

The main objective of this work is to obtain tractable solutions to allow for further parametric studies. Stress and displacement solutions in the analytical solution form are presented in FGM thick-walled cylinders with exponentially-varying elastic modulus in the radial direction. Although the case of FGM cylinders with variation of elastic properties obeying a simple power law is extensively studied, the results for exponentially varying properties are scarcely available in the literature. A positive inhomogeneity constant refers to increasing stiffness in the radial direction.

We consider a thick cylinder whose elasticity modulus varies in radial direction and has the following characteristics: $R_{in} = 0.1$ m, $R_{out} = 0.2$ m. The elasticity modulus, is taken $E_i = 200$ GPa. The Poisson's ratio has a constant value $\nu = 0.3$.

The applied internal and external pressures are $P_i = 500$ MPa and $P_o = 0$ MPa, respectively. The constant of the inhomogeneity parameter can be adjusted in various ways to reproduce various conditions. However, the study was conducted for different values of inhomogeneity parameter $\alpha = -2, -1, 0, 1$ and 2 .

We compared the results of our analyses with the results obtained from finite element method (FEM). A finite element model of the pressure vessel subjected to internal pressure was constructed using FE code. The geometry is axisymmetric. Consequently, half of cylindrical specimen was considered. Thus, we reduce the number of nodes and the computational time. In order to consider the radial continuous varying of the elastic modulus along the thickness of hollow cylinder with special function, the exponential expression of Young's modulus (Eq. (1)) was implemented into the FE model.

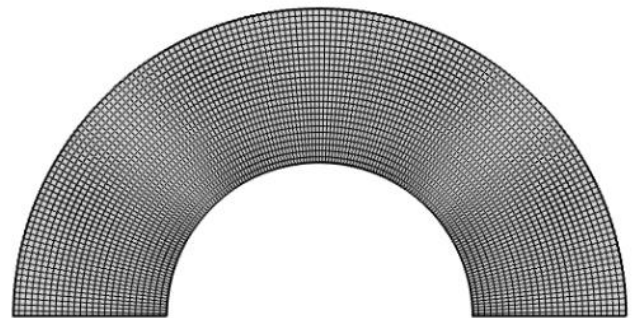


Figure 2. Numerical model geometry.

Internal and external pressures are applied to the nodes of inner and outer layers, respectively. The boundary condition and mesh distribution of the FE model employed in this study is presented in Fig. 2.

For different values of inhomogeneity parameter $\alpha = -2, -1, 0, 1$ and 2 , dimensionless modulus of elasticity across the radial direction is plotted in Fig. 3. According to this figure, at the same radial position r in $R_{in} < r < R_{out}$, dimensionless modulus of elasticity increases as the parameter of inhomogeneity α increases.

For different values of α , the distribution of the radial displacement resulted from the analytical solution across the thickness of a cylinder is depicted in Fig. 4. It was obviously observed in Fig. 4 that the radial displacements have its maximum values in internal surface ($r = R_{in}$). The radial displacement values decrease gradually from inner surface through the outer surface. We observe an increase of the displacement with the decrease of α . The increase in radial displacement with the decrease of α is due to the fact that the global stiffness of the cylinder decreases.

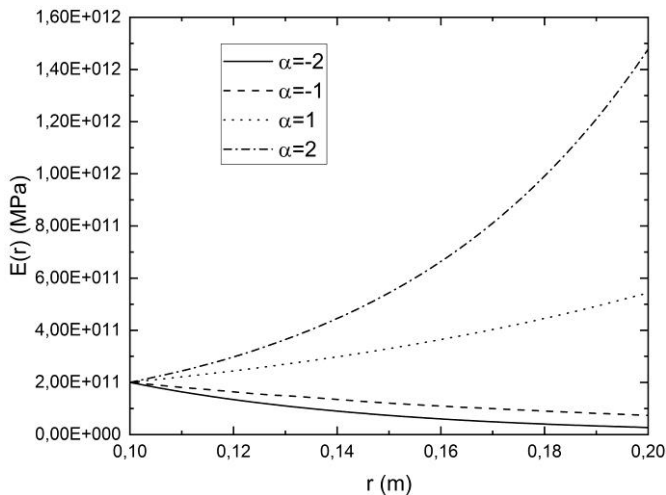


Figure 3. Radial distribution of elastic modulus for different values of inhomogeneity parameter.

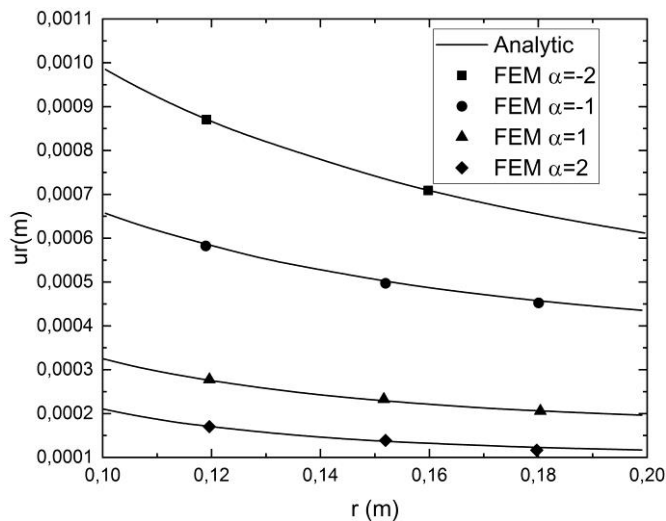


Figure 4. Radial distribution for radial displacement for different values of inhomogeneity parameter.

The radial stress was plotted in Fig. 5 for different values of inhomogeneity parameter $\alpha = -2, -1, 1$ and 2 . The variation in the radial stress of heterogeneous material is similar to that of homogenous material.

For all values of α considered, the magnitude of the radial stress has a monotonic behavior increasing in r . It was seen that, for each fixed r in $R_{in} < r < R_{out}$ the radial stress magnitude decrease as α increases. It is due to the fact that the global stiffness of the cylinder increases. Increasing the inhomogeneity constant causes an increase in the stresses.

The circumferential stress was plotted along the radial direction and shown in Fig. 6. The hoop stress along the radius decreases monotonically respect to r for all different negative values of α considered (similar to thick cylinders made of isotropic materials), while the hoop stress increases respect to r for positive values of α . It was seen that, for each fixed value of r in $r < 0.14$ m, the hoop stress magnitude decrease as α increases. However, for each fixed value of r in $r > 0.14$ m, the hoop stress magnitude increase as α increases. Indeed, higher values of α mean increasing stiffness.

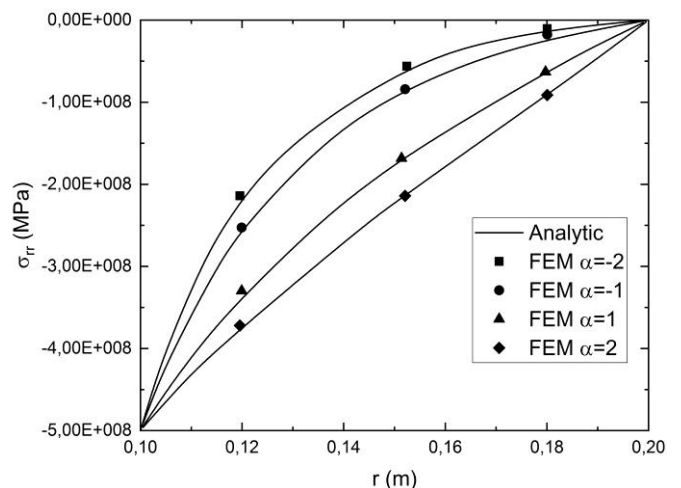


Figure 5. Radial distribution of radial stress for different values of inhomogeneity parameter α .

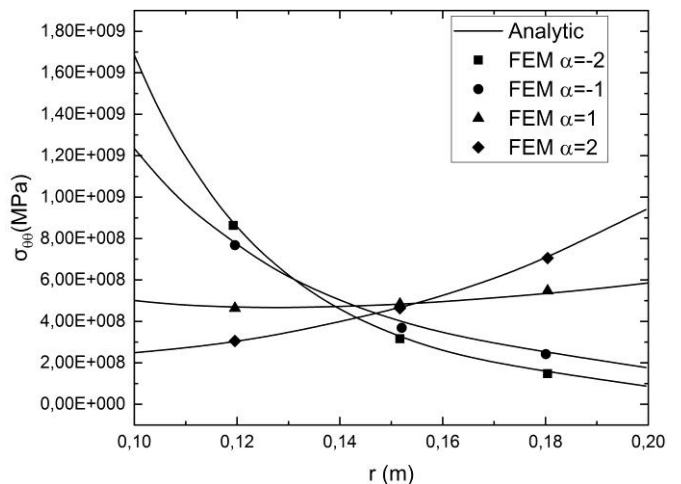


Figure 6. Radial distribution of hoop stress for different values of inhomogeneity parameter α .

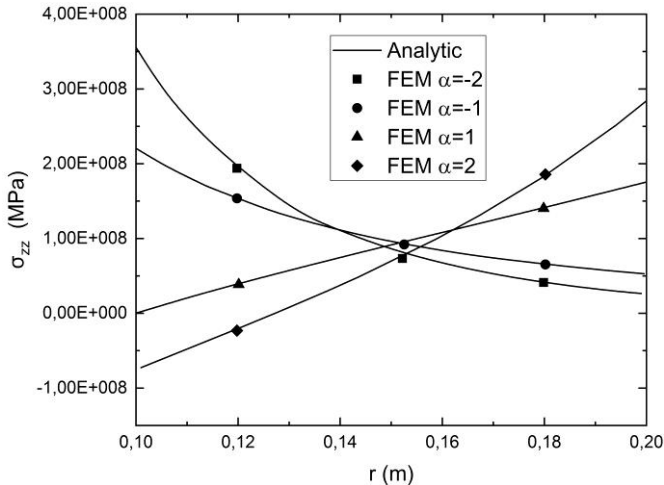


Figure 7. Radial distribution of axial stress for different values of inhomogeneity parameter α .

Fig. 7 shows the axial stress distribution plotted along the radial direction. The axial stress along the radius decreases monotonically respect to r for all different negative values of α considered, while the hoop stress increases respect to r for positive values of α .

It was seen that, for each fixed value of r in $r < \sim 0.15$ m, the axial stress magnitude decrease as α increases. However, for each fixed value of r in $r > \sim 0.15$ m, the hoop stress magnitude increase as α increases. Indeed, higher values of α mean increasing stiffness.

V. Conclusions

In this work, an analytical formulation was presented to find displacements and stress components in thick-walled cylinder subjected to internal pressure. The FGM properties were supposed to be exponentially-varying across the thickness of the cylinder.

For validation, a finite element (FE) model of the pressurized cylinder was constructed, where the radial continuous varying of elastic modulus along the thickness was implemented in a FE code. Then we compared the analytical and numerical solutions. The analytical solution was validating since the comparisons of the numerical results with solutions obtained gives a good agreement.

The results are presented as evolution of the displacement and stress components through the radial direction are plotted for different material inhomogeneity parameter. From above results, it can be concluded that the spatial variation of Young's modulus has a great effect on stresses and radial displacement distribution in FGM cylinder. Thus, the parameter of inhomogeneity is a useful parameter from a design point of view and can be tailored to specific applications to control the stress distributions.

References:

1. V. Birman and L. W. Byrd Modeling and analysis of functionally graded materials and structures. *Appl Mech Rev*, 60, 195–216, 2007.
2. F. Ubertini, G. Comanducci, N. Cavalagli, et al. Environmental effects on natural frequencies of the San Pietro bell tower in Perugia, Italy, and their removal for structural performance assessment. *MechSyst Sig Process*, 82, 307–322, 2017.
3. V.V. Rao, Krishna K. Veni and P.K.Sinha Behavior of composite wing T-joints in hygrothermal environments. *Aircr Eng Aerosp Tec*, 76, 404–413, 2004.
4. K. Celebi, D. Yarimpabuc, I. Keles. A novel approach to thermal and mechanical stresses in a FGM cylinder with exponentially varying properties. *Journal of theoretical and applied mechanics*, 55, 343–351, 2017.
5. Z. M. Nejad, M. Jabbari, and A. Hadi. A review of functionally graded thick cylindrical and conical shells. *Journal of Computational Applied Mechanics*, 48, 2, 357–370, 2017.
6. M. Hosseini, M. Shishesaz, and A. Hadi. Thermoelastic analysis of rotating functionally graded micro/nanodisks of variable thickness. *Thin-Walled Structures*, 134, 508–523, 2019.
7. A. Lal, and K. Markad, Thermo-Mechanical Post Buckling Analysis of Multiwall Carbon Nanotube-Reinforced Composite Laminated Beam under Elastic Foundation. *Curved and Layered Structures*, 6, 1, 212–228, 2019.
8. M. Ghannad, G.H. Rahimi, M.Z. Nejad, Elastic analysis of pressurized thick cylindrical shells with variable thickness made of functionally graded materials. *Composites: Part B* 45 388–396, 2013.
9. R. Sburlati. Analytic elastic solutions for pressurized hollow cylinders with internal functionally graded coatings. *Composite structures*, 94, 3592–3600, 2012.
10. M., Jabbari, S., Sohrabpour, M.R., Eslami. Mechanical and thermal stresses in a functionally graded hollow cylinder due to radially symmetric loads. *International Journal of Pressure Vessels and Piping*, 79, 493–497, 2002.
11. K. Abrinia, H. Naei, F. Sadeghi and F. Djavanroodi. New Analysis for The FGM Thick Cylinders Under Combined Pressure and Temperature Loading. *American Journal of Applied Sciences*, 5, 7, 852–859, 2008.
12. N. Tutuncu, M. Ozturk. Exact solutions for stresses in functionally graded pressure vessels. *Compos B Eng* 32, 8, 683–686, 2001.
13. M.Z. Nejad, P. Fatehi. Exact elasto-plastic analysis of rotating thick-walled cylindrical pressure vessels made of functionally graded materials. *Int J EngSci* 86, 26–43, 2015.
14. Y.Z. Chen, X.Y. Lin. An alternative numerical solution of thick-walled cylinders and spheres made of functionally graded materials. *Comput Mater Sci* 48:640–647, 2010.
15. G.J. Nie, Z. Zhong, R.C. Batra. Material tailoring for functionally graded hollow cylinders and spheres. *Compos Sci Technol* 71, 5, 666–673, 2011.
16. G.J. Nie, R.C. Batra. Exact solutions and material tailoring for functionally graded hollow circular cylinders. *J. Elast.* 99, 179–201, 2010.

17. N. Tutuncu, Stresses in thick-walled FGM cylinders with exponentially-varying properties, *Eng. Struct.* 29, 2032–2035, 2007.
18. Y.Z. Chen, X.Y. Lin, Elastic analysis for thick cylinders and spherical pressure vessels made of functionally graded materials, *Comput. Mater.Sci.* 44, 581–587, 2008.
19. E.E. Theotokoglou, I.H. Stampouloglou, The radially nonhomogeneous elastic axisymmetric problem, *Int. J. Solid Struct.* 45, 6535–6552, 2008.
20. A. Benslimane, R. Benchallal, S. Mammeri, M. Methia, &M.A. Khadimallah. Investigation of displacements and stresses in thick-walled FGM cylinder subjected to thermo-mechanical loadings. *International Journal for Computational Methods in Engineering Science and Mechanics*, 22(2), 138-149, 2020.
21. A. Benslimane, C. Medjdoub, M. Methia, M.A. Khadimallah, & D. Hammiche. Investigation of displacement and stress fields in pressurized thick-walled FGM cylinder under uniform magnetic field. *Materials Today: Proceedings*, 36, 101-106, 2021.
22. R. Benchallal, A. Benslimane, O. Bidgoli, &D. Hammiche. Analytical solution for rotating cylindrical FGM vessel subjected to thermomechanical loadings. *Materials Today: Proceedings*, 53, 24-30, 2022.
23. M. Ghannad, H. Gharooni. Elastic analysis of pressurized thick FGM cylinders with exponential variation material properties using TSDT. *Lat Am J Solids Struct* 12, 6,1024–1041, 2015.
24. Y.Z. Chen, X.Y. Lin. Elastic analysis for thick cylinders and spherical pressure vessels made of functionally graded materials. *Comput Mater Sci* 44, 2, 581–587, 2008.
25. H.L. Dai, Y.N. Rao, T. Dai. A review of recent researches onFGM cylindrical structures under coupled physical interactions, 2000–2015. *Compos Struct* 152, 199–225, 2016.
26. Abramowitz M. and Stegun AI, *Handbook of a thematical functions*. Dover Eds; 1970.